



**ESTIMATED SEDIMENT YIELD FROM COASTAL LANDSLIDES AND
ACTIVE SLOPE DISTRIBUTION ALONG THE BIG SUR COAST**

and

Addendum: Coastal Cliff Erosion Rates, Big Sur, CA

**A Report of Findings for the
COASTAL HIGHWAY MANAGEMENT PLAN
CALIFORNIA DEPARTMENT OF TRANSPORTATION, DISTRICT 5**

**Prepared by
C. Hapke^{1,2}
K. Dallas²
K. Green²**

**¹U.S. GEOLOGICAL SURVEY, PACIFIC SCIENCE CENTER
and**

²UNIVERSITY OF CALIFORNIA, SANTA CRUZ

May 2003



TABLE OF CONTENTS

EXECUTIVE SUMMARY	3
INTRODUCTION	4
PURPOSE	6
STUDY AREA	6
Geologic Setting	8
Climate and Waves	11
METHODS	12
Photogrammetry	12
GIS	15
Error Analysis	17
SEDIMENT YIELD FROM COASTAL LANDSLIDES	18
ACTIVE SLOPE DISTRIBUTION	19
APPLICATIONS AND LIMITATIONS	21
SUMMARY	22
ACKNOWLEDGEMENTS	24
REFERENCES	24
SEDIMENT YIELD MAPS 1-3	27-29
ADDENDUM	30
Executive Summary	30
Introduction	31
Methods	34
Coastal Cliff Retreat	35
Summary	35
References	36
Cliff Retreat Rate Maps 1-9	37-45

EXECUTIVE SUMMARY

Along the Big Sur coastline in central California, the rugged Santa Lucia Mountains descend abruptly into the Pacific Ocean, creating one of the most extreme coastal slopes in the conterminous United States. Coastal Highway 1 runs along the edge of the coastal slope, and the waters adjacent to the Big Sur coastline are within the Monterey Bay National Marine Sanctuary (MBNMS), a protected area of coastal waters and home to a variety of aquatic species. Weak rocks and steep topography provide ideal conditions for frequent large landslides that contribute to the littoral sediment budget. Little is known about the nearshore sediment budget in this area, including the amount, rate and frequency of input to the system from coastal landslides. Landslide material provides protection from waves at the base of the slope, and sediment entering the water provides nutrients and material for various nearshore habitats. Anthropogenic disposal of landslide material (from road maintenance) may upset the equilibrium of the system through burial of organisms and/or alteration of bottom type (e.g. conversion of rocky substrate to soft bottom). However restricting any disposal may starve a system of necessary nutrients and sediments.

The focus of this study is to provide an estimate of the historical volume of sediment (sediment yield) that enters the littoral system directly from coastal slope failures, and to map the spatial and temporal distribution of active coastal slopes. The purpose is to provide background data for the Coast Highway Management Program and to advance the fundamental understanding of coastal landslide input rates and processes along this stretch of coastline.

The sediment yield is derived by applying digital photogrammetric and GIS techniques to create 3D topographic models. Stereo-pairs of aerial photographs from two time periods (1942, 1994) spanning 52-years are used to create digital terrain models (DTMs) of nine discontinuous sections of the coast. The DTMs represent the topographic surface at the moment the photographs were taken. The volume change is estimated by subtracting the topography of one time period from the other. In areas where the volumes could not be directly estimated due to poor data quality, the sediment yield is interpolated based on similarities in geology along-coast. The sediment yield maps presented in this study are 'strip maps' that show the variation in the estimated and interpolated sediment yield as a coast-parallel strip representing the sediment yield from the corresponding stretch of subaerial coastal slope.

In addition to the sediment yield estimation, the maps also show the spatial and temporal distribution of active slopes, again as strips parallel to the coastline. Each of the three active slope strips represents the along-coast extent of areas where subaerial active slopes were identified for a particular date of aerial photography. The active slope mapping was conducted by georeferencing images from 1929, 1942 and 1994 and digitizing the areas of active slope failure based on bare surfaces and lack of vegetation visible in the images.

The sediment yield appears to be closely related to the variable geology, as mapped in detail by Wills *et al.* (2001). In general, the areas of lowest sediment delivery are in the stronger

granitic rocks that are concentrated along the northern portion of the Big Sur area. The highest rates are within the weak Franciscan Complex rocks that dominate in the central and southern portions of the coastline. The sediment yields range from $1,000 \pm 100 \text{ m}^3/\text{km}/\text{yr}$ ($2,100 \pm 350 \text{ yd}^3/\text{mi}/\text{yr}$) to a high of $46,700 \pm 4,800 \text{ m}^3/\text{km}/\text{yr}$ ($61,100 \pm 6,300 \text{ yd}^3/\text{mi}/\text{yr}$). The active slope distribution mapping indicates that there are specific areas where the slopes have been active throughout the time period of the distribution analysis, such as in the area around Lucia.

INTRODUCTION

The 1982-83 and 1997-98 El Niños brought very high precipitation to California's central coast, raising groundwater levels and destabilizing slopes throughout the region. A number of large landslides in the coastal mountains of Big Sur in Monterey and San Luis Obispo counties blocked Coast Highway 1, closing the road for months at a time. Large slope failures such as these are common along the Big Sur coast section of Highway 1 due to the steep topography and weak bedrock (Fig. 1). A large slope failure in 1983 resulted in the closure of Highway 1 for over a year for repairs and slope stabilization. Highway repairs from the 1983 landslide cost over \$7 million and generated a combined three million cubic yards of debris from landslide removal and excavations to re-establish the highway (Engellenner, 1984).

The California Department of Transportation (Caltrans) is responsible for maintaining the Highway 1 corridor and for providing prompt and safe access for both local residents and tourists. Prior to the establishment of the marine sanctuary, 'typical road opening measures' sometimes involved disposal of some landslide material and excess material generated from slope stabilization onto the seaward side of the highway. It is inferred that some or most of this disposed material, either directly, or indirectly through subsequent erosion, was eventually transported downslope into the adjacent ocean. In addition to the landslides that initiate above the road, natural slope failures also occur on the steep slopes below the road, delivering material to the base of the coastal mountains where it is eroded and dispersed by waves and nearshore currents. As a result, any coastal slope landslide, whether through natural or anthropogenic processes, can result in sediment entering the littoral zone. The waters offshore of the Big Sur coastline are part of the Monterey Bay National Marine Sanctuary (MBNMS) (Fig. 2), which was established in 1992. At this time, Caltrans landslide-disposal practices along the Big Sur coast came under question for several reasons. The U.S. Code of Federal Regulations, Title 15,



Figure 1: Large-scale landslides are common along the Big Sur coast and road closures from slides are common. This photo shows a section of Highway 1 after the repair of the Hurricane Point landslide (PM 58.0). Photo courtesy of Caltrans.

Section 922.132 (NOAA, 2002) prohibits discharging or depositing, from beyond the boundary of the Sanctuary, any material or other matter that subsequently enters the Sanctuary and injures a Sanctuary resource or quality. The landslide disposal practices previously used by Caltrans had the potential to alter nearshore zone habitat by converting marine habitats from rocky substrate to soft bottom. In addition, the disposal practices had the potential to increase nearshore zone suspended sediment concentrations, possibly impacting coastal biological communities. On the other hand, natural mass wasting processes including coastal cliff erosion, coastal landslides and streams deliver sediment to the coast in unknown quantities, providing

nutrients as well as source material for beaches. Road maintenance and repair practices along the Highway 1 corridor may act to reduce sediment input relative to natural processes.

PURPOSE

The purpose of this study is to quantify the long-term volume of sediment entering the nearshore system from coastal mass wasting, including landslides and cliff erosion, along the approximately 120-km-long (75-mi) Big Sur coast from south of the Carmel River to San Carpoforo Creek (Fig. 2). The geographic limits of the study correspond to that portion of the coast where the steep slopes of the Santa Lucia Mountain Range descend uninterrupted to the Pacific Ocean, and where data could be derived. The primary goals of the research are to quantify the volume of sediment that enters MBNMS through coastal landslide processes using historical and recent aerial stereo photographs, to map the temporal and spatial variations in landslide distribution along the coast, and to relate the volume losses to the complex geology of the region in order to document the geological controls on sediment yield from coastal landslides. The Coast Highway Management Plan (CHMP) was established with the intention of developing highway management approaches and solutions collaboratively with the MBNMS. This study was undertaken as a direct result of the identification that there was a fundamental lack of data on background sediment volumes entering the Sanctuary from coastal landslides. As a result, Caltrans committed resources through the CHMP to support the necessary research activities related to filling data gaps.

STUDY AREA

The Big Sur coastline lies on the western boundary of the Coast Range, a northwest-trending series of mountains and valleys flanking the coast from near Santa Barbara, CA to the Oregon border. In the Big Sur area, the Santa Lucia Mountain Range reaches elevations of nearly 1600 m (1 mi) within five km (three miles) of the coast, making this one of the steepest coastal slopes in the conterminous United States.

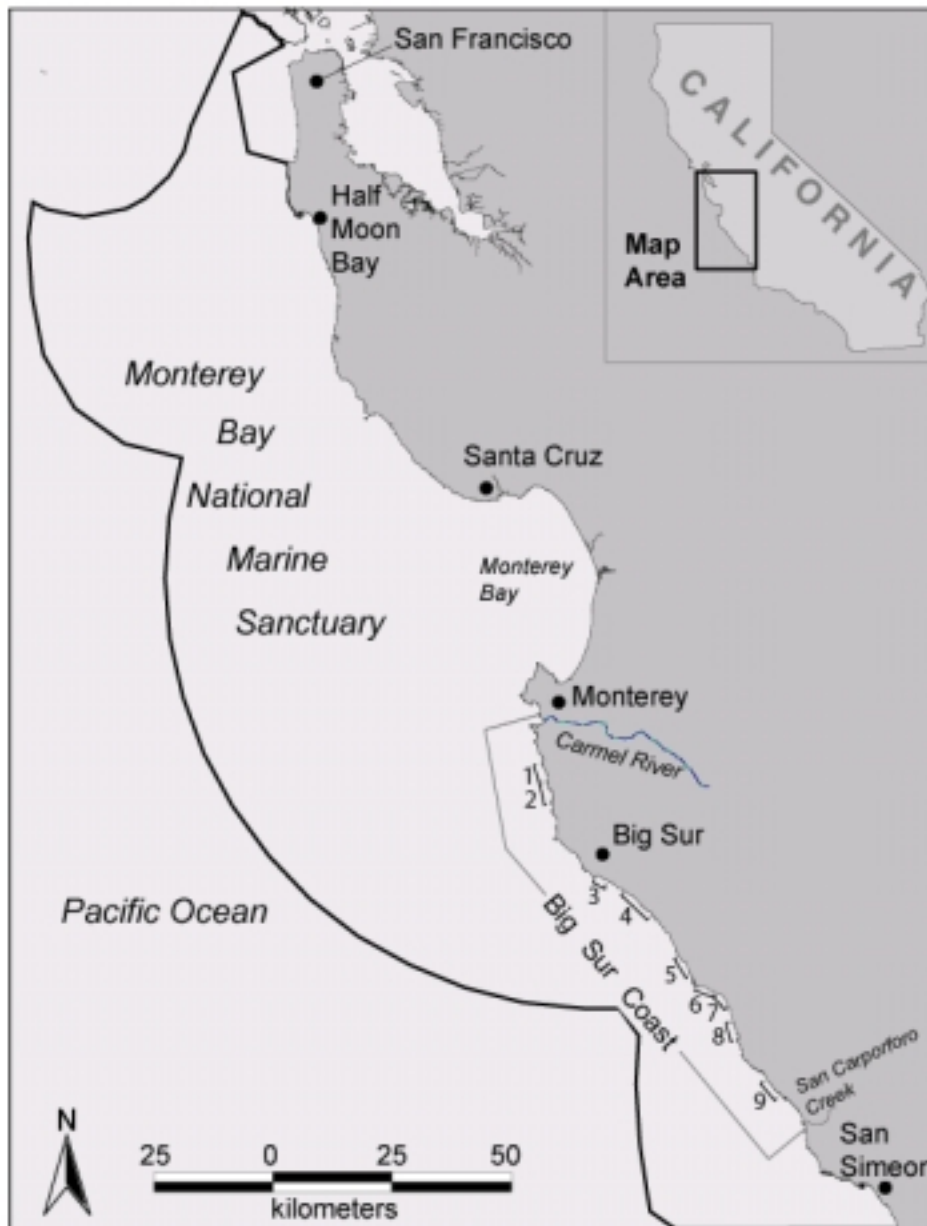


Figure 2: Map showing location of the MBNMS and the Big Sur coast in central California. The numbers 1-9 shown on the map correspond to the specific study sections.

Geologic Setting

The rocks exposed along the Big Sur coastline are a complex mixture of sheared and metamorphosed sedimentary and igneous rocks of the Late Jurassic to Miocene Franciscan Complex, and early Mesozoic plutonic and metamorphic rocks of the Sur complex (Dibblee, 1974; Ross, 1976; Hall, 1991). The Franciscan Complex is found along much of the California coast, and records a period of time prior to 30 million years ago when the active plate boundary between the North American and Pacific plates was convergent rather than the present day strike-slip. The rocks of the Franciscan Complex are considered to be the remains of an ancient accretionary wedge that formed when oceanic plate material along with overlying oceanic sediments were scraped up as the Farallon plate was subducted beneath the North American plate (Blake *et al.*, 1988). These rocks were subsequently transported northward along the San Andreas Fault Zone (SAFZ) to their present position. The predominant Franciscan Complex rock types exposed along the Big Sur coastline in the study areas include metavolcanic rocks (greenstone), serpentinite, and interbedded, highly sheared argillite and greywacke (Bailey *et al.*, 1964). Study location sections 3, and 6-9 (Table I; Figures 2 and 3) are within the Franciscan Complex.

The 130 million-year-old plutonic rocks of the Sur complex (James and Mattinson, 1988) form the core of the Salinian block which is bounded on its east side by the San Andreas fault, and to the west by the Sur-Nacimiento fault. The granitic and metamorphic rocks of the Salinian block represent a portion of the ancestral Sierra Nevada range that has been transported along the SAFZ to its present position in central California (Page, 1982). The Sur complex rocks exposed in study sections 1 and 2 (Table I; Figures 2 and 3) are quartz diorite and charnockitic tonalite, respectively (Compton, 1966; Ross, 1976).

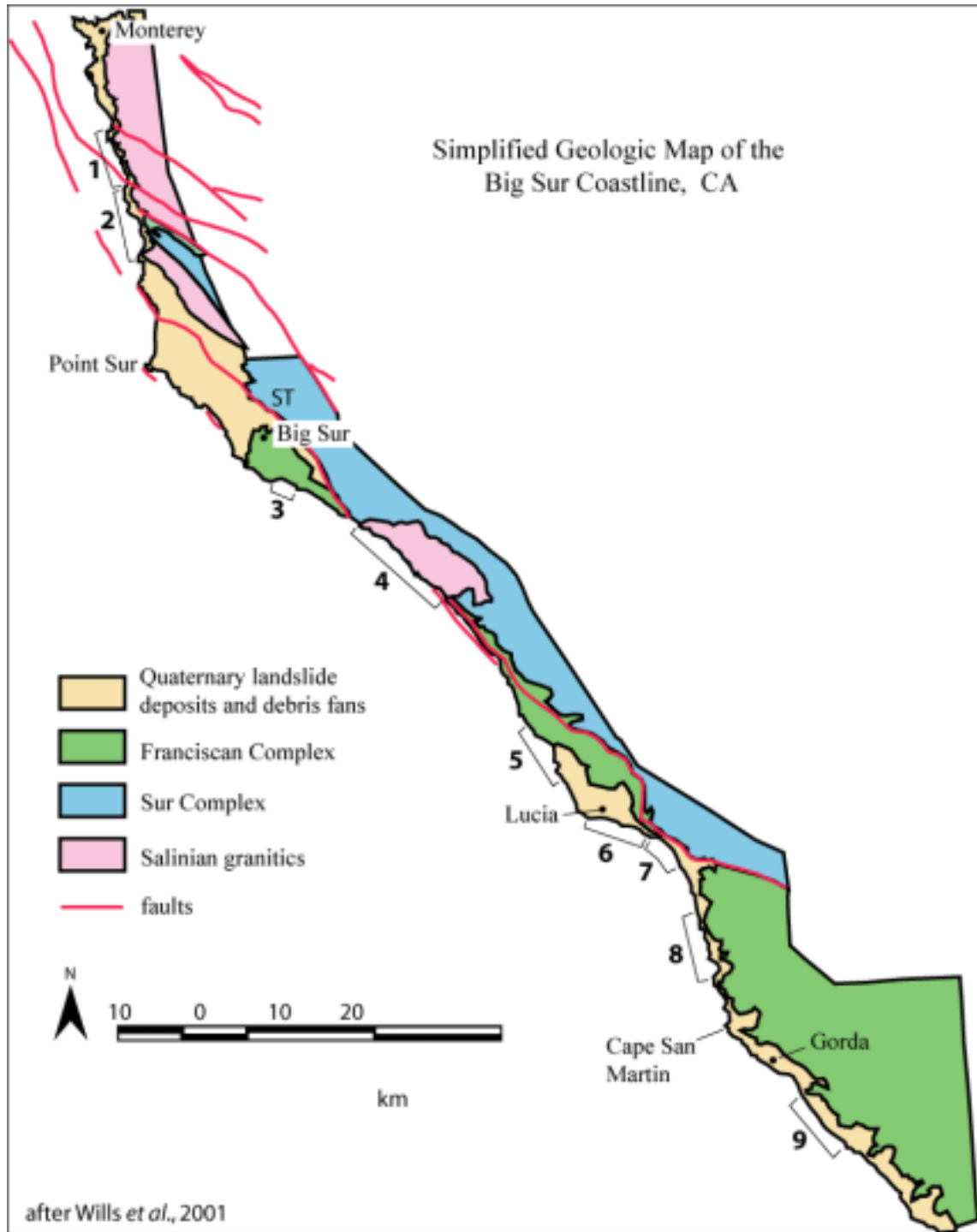


Figure 3: Geologic Map of the Big Sur coast area showing the general lithologies exposed along the coast. Major faults are shown as red lines. The numbers 1 – 9 are the locations of the specific study areas.

TABLE 1: GEOLOGIC UNITS FOUND IN EACH OF THE STUDY AREAS (from mapping by Wills, *et al.*, 2001)

Section No.	Post mile	Primary (I) and secondary (II) geologic unit	Description* (after Wills, <i>et al.</i> , 2001)
1	63.1 - 66.0	I. Kqd	Cretaceous hornblende-biotite quartz diorite: medium to dark gray coarse-grained
		II. Qdf	Debris fan deposits; nearly continuous and overlapping.
2	59.5 – 63.0	I. Kqd	Cretaceous hornblende-biotite quartz diorite.
		I. KMct	Charnockitic tonalite: dark greenish gray, coarse-grained; very fractured and sheared.
3	45.6 – 46.6	II. Qdf	Debris fan deposits; nearly continuous and overlapping.
		I. KJf	Undifferentiated Franciscan Complex
4	36.8 – 41.5	II. Qls	Landslide deposits; discontinuous.
		I. KMct	Charnockitic tonalite
5	26.0 – 29.2	II. Qls	Landslide deposits; discontinuous.
		I. KJf	Franciscan Complex (mélange)
6	21.3 – 24.1	II. Qls	Landslide deposits; continuous and overlapping.
		I. KJf	Franciscan Complex (mélange)
7	19.4 – 21.2	I. KJf	Franciscan Complex (mélange)
		II. Qls	Landslide deposits; continuous and overlapping.
8	14.0 – 17.4	I. KJf	Franciscan Complex (mélange)
		II. Qls	Landslide deposits; continuous and overlapping.
9	73.0 (SLO) – 3.5 (MON)	I. KJf	Franciscan Complex (mélange)
		II. Qls	Landslide deposits; continuous and overlapping.

*A rock type is only described the first time it is listed in the table.

**Post miles are for Monterey County unless otherwise denoted

The Salinian and Franciscan bedrock is overlain in many areas by a relatively thick blanket of debris fan material composed of poorly bedded silts and sands and beds of angular cobbles and boulders; much of the original bedrock geology is also disrupted by numerous landslide deposits (Hall, 1991; Wills *et al.*, 2001).

The rocks of the Franciscan Complex tend to be weaker than those of the Sur complex; the majority of the chronic landslides occur where Franciscan Complex rocks underlie the steep slopes. However, the lithology within the Franciscan Complex varies dramatically, and the

softer, highly sheared rocks and mélangé are more prone to landsliding whereas the various sedimentary strata and volcanic rocks form somewhat more stable slopes.

Climate and Waves

The Big Sur region of California, like much of central California, experiences a Mediterranean climate, with most precipitation falling in the winter months, and mild temperatures throughout the year. The weather in the region is predominantly controlled by the North Pacific High: its presence in the summer produces dry westerly winds and upwelling of fog-producing cold ocean water, and its absence in the winter results in high rainfall concentrated in a period of several months (October through May)(Gilliam, 1962). Rainfall amounts vary with elevation. Lower slopes near the coast may receive less than half the rainfall that falls near the top of the mountains. The average annual rainfall near the town of Big Sur from 1914 to 1987 was 109 cm (43 in); it is estimated that approximately 230 cm (92 in) falls higher on the slopes (Henson and Usner, 1993),

Much of the Big Sur coastline is directly exposed to Pacific storms. Waves reach the base of the coastal slope along the entire coast except where a few larger pocket-beaches have formed. The continental shelf is considerably narrower along the Big Sur coast to the north or south, narrowing from approximately 16 km (9.6 mi) near Santa Cruz, to less than 5 km (3 mi) south of Monterey (California Coastal Commission, 1987). Since the water depth is approximately the same at the edge of the shelf, the shelf is steeper along the Big Sur coast. As a result, there is less dissipation of deep-water wave energy as waves travel across the shelf (Komar, 1998), and thus waves encounter the shoreline with considerably higher energy than where the shelf is more gently sloping.

For most of the year, swells along this portion of the coast are from the northwest. Data from the NOAA National Data Buoy Center shows average significant wave heights at Cape San Martin (see Fig. 3) of 9 m (30 ft) in the winter months of January and February. Wave periods in the winter average 18 seconds. The mean tide range along the Big Sur coast is 1.3 m (4.1 ft), with a diurnal range of 1.7 m (5.3 ft) (California Coastal Commission, 1987).

METHODS

The primary tools used in this study are digital photogrammetry and GIS. Digital photogrammetry involves the processing of historical and recent vertical aerial photographs to produce Digital Terrain Models (DTMs) from 3D stereo models. Time-sequence DTMs are brought into a GIS where volume changes are calculated, and the spatial distribution of the terrain changes can be analyzed and compared to the local geology. The historical aerial photographs chosen for this study are from 1942 (1:30,000) whereas the recent photographs are from 1994 (1:24,000). These photographs provide the base for determining a 52-year end-point volumetric change for the nine sections of coast. These particular aerial photographs were chosen based on the appropriateness of scales of photographs that could provide regional coverage of the coastline, a length of time between the photographic series to ensure the longest possible time period for the long-term rate calculation, and the availability of stereo film positives (diapositives) to minimize non-systematic errors.

Digital Photogrammetry

Digital photogrammetry requires a specific workflow that results in the production of orthophotographs (digital images from which all displacements have been removed) and DTMs (Fig. 4). To create true orthophotographs, displacements inherent in unrectified photography must be corrected in order to make accurate measurements from the images. The displacements include those related to the camera system, the camera position, and the terrain relief in the area (Slama, 1980; Falkner, 1995; Wolf and Dewitt, 2000). Interior orientation adjusts the images according to the camera system by incorporating known calibrated information from the camera such as the focal length, radial lens distortion, and distance between fiducial points. Exterior orientation corrects for changes in the position of the sensor platform through a series of points that tie a strip of images to one another in image space and uses ground control point data along with aerotriangulation to perform a best-fit mathematical transformation to assign real-world coordinates to the images.

Once the interior and exterior orientations have been applied, the resulting images are pseudo-orthorectified. However, accurate measurements cannot be made until the effects of relief

displacement are removed, which is especially crucial in a high relief terrain such as Big Sur. Removal of relief displacement requires the creation and incorporation of a DTM. The DTMs in this study are built from the stereo images using a Triangulated Irregular Network (TIN) of elevation points rather than a standard grid model in order to best capture the steep and rapidly changing topography (Hapke and Richmond, 2000; Maune *et al.*, 2001). TINs and grids are simply different ways of storing and representing data in a DTM or a DEM (digital elevation model), respectively.

Prior to photogrammetric processing, the original film diapositives acquired for this study were converted to digital format by scanning at high resolution (approximately 1200 dpi) with a photogrammetric scanner. The images are next imported into commercial photogrammetry software to perform all corrections and to create and edit the TIN while viewing in stereo. Stereo-viewing capabilities ensure the accurate placement of breaklines and allow the removal or adjustment of erroneous data points, including those on buildings, vegetation, and in the water.

For modern digital photogrammetric processing that requires high accuracy, ground control points for orthorectification are usually photo-identifiable points that are surveyed in the field using a differential global positioning system (DGPS). Given the nature of this study, in which it is necessary to produce DTMs of large stretches of remote coastline, ground surveying was impractical for collection of ground control points. In lieu of ground survey data, ground control points for the recent (1994) aerial photography were derived from USGS Digital Orthoquadrangles (DOQs)(for horizontal control) and 30 m National Elevation Data that were vertically adjusted using supplemental ground survey data to improve vertical resolution (for vertical control). The errors associated with these control data are incorporated into the overall model error analysis outlined in the *Error Analysis* section below.

Obtaining ground control data for historical photography, especially in a relatively undeveloped and remote area such as Big Sur, presents additional challenges in the creation of orthophotographs and DTMs. For this study, the recent (1994) images are rectified and a DTM is created prior to the processing of the historical (1942) images. The recent images and resulting DTM are then used to derive the control for the 1942 images. In many cases the

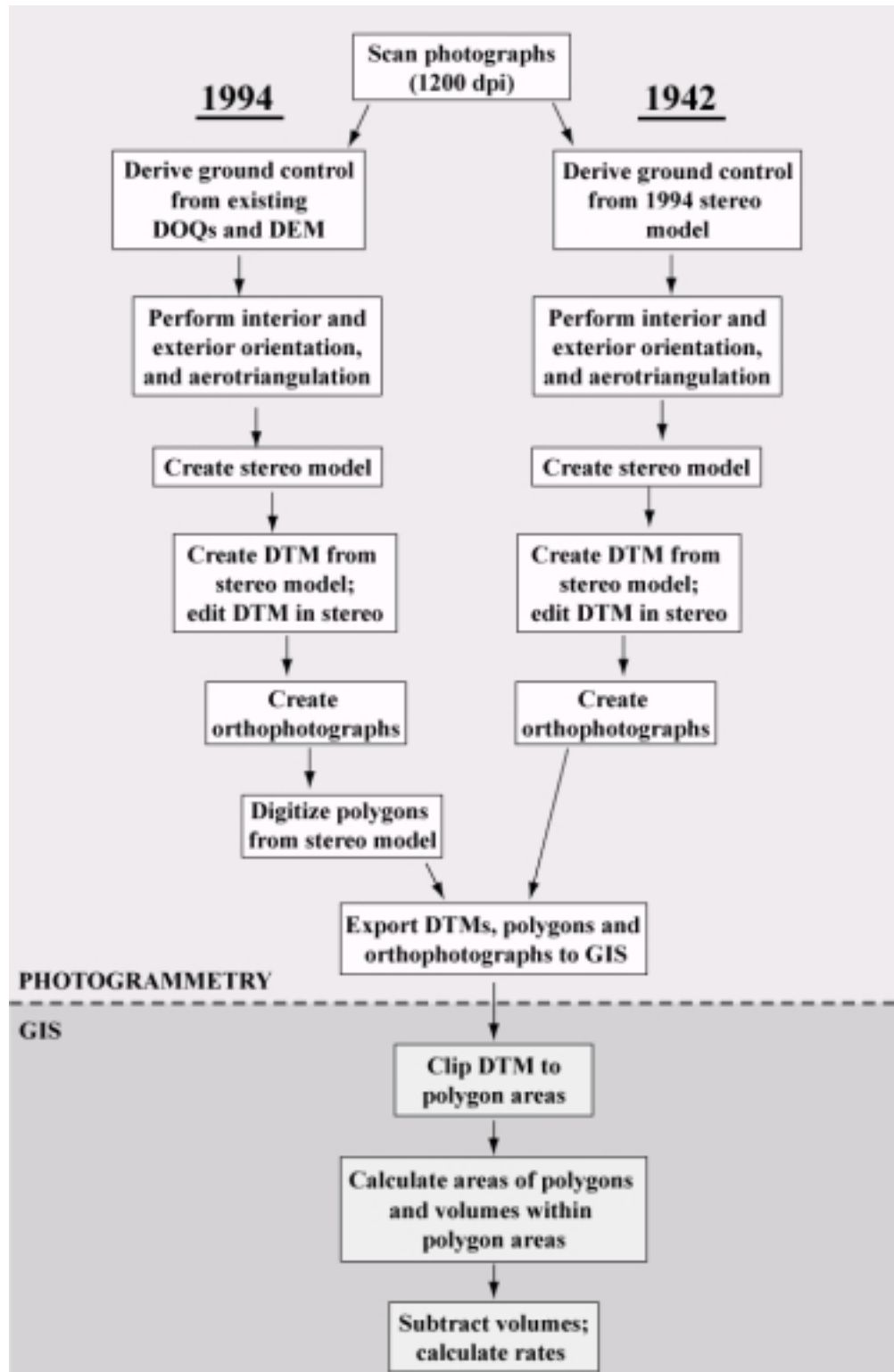


Figure 4: Procedure for the production of DTMs and the calculation of volumetric change using photogrammetry and GIS.

extrapolated control includes features such as individual rocks in rock outcrops that appear to be stable in the period between photographs, as well as features associated with road intersections, driveways, and parking lots. Thus, the historical model is rectified *relative* to the recent model; this improves the overall accuracy by allowing for a sufficient number and distribution of ground control points. Since the objective of the study is to determine the change from one period to the next, the relative change between the two surface models accurately represents the differences.

A final step prior to exporting the orthophotomosaics and the DTMs from the photogrammetry software is to determine the areas for each section under which the volumes will be calculated (Fig. 5). This is completed within the photogrammetry software so that the 3D viewing capabilities of the software can be utilized to digitize polygons that accurately represent natural breaks in the terrain. As this study was designed to determine the volumetric input to the nearshore directly from coastal landslides, the polygons do not include any major drainages which extend upland beyond the first ridge crest. Furthermore, the polygon perimeters outline topographic breaks that define the direct coastal slope, or that slope along which material in motion would most likely travel directly to the base of the slope, and not into an adjacent drainage (Fig. 5). Because the determination of the polygons involves distinguishing topographic breaks, stereo-viewing capabilities are essential.

Geographic Information Systems (GIS)

Once the topographic surface models are generated and edited, they are exported from the photogrammetry software and into a GIS. The orthophotomosaics and delineated polygons generated for each study section are also brought into GIS, and all layers including other existing data sets such as geologic maps and field data maps can be viewed and analyzed in real world coordinates. GIS provides a number of tools that can be used to conduct detailed terrain analyses, including volume calculations, slope analyses, and contouring of various data sets.

The volume for each topographic surface model is calculated from the two dates, above a datum of 1.0 m (3.1 ft) above mean sea level. The 1.0 m (3.1 ft) elevation represents the lowest

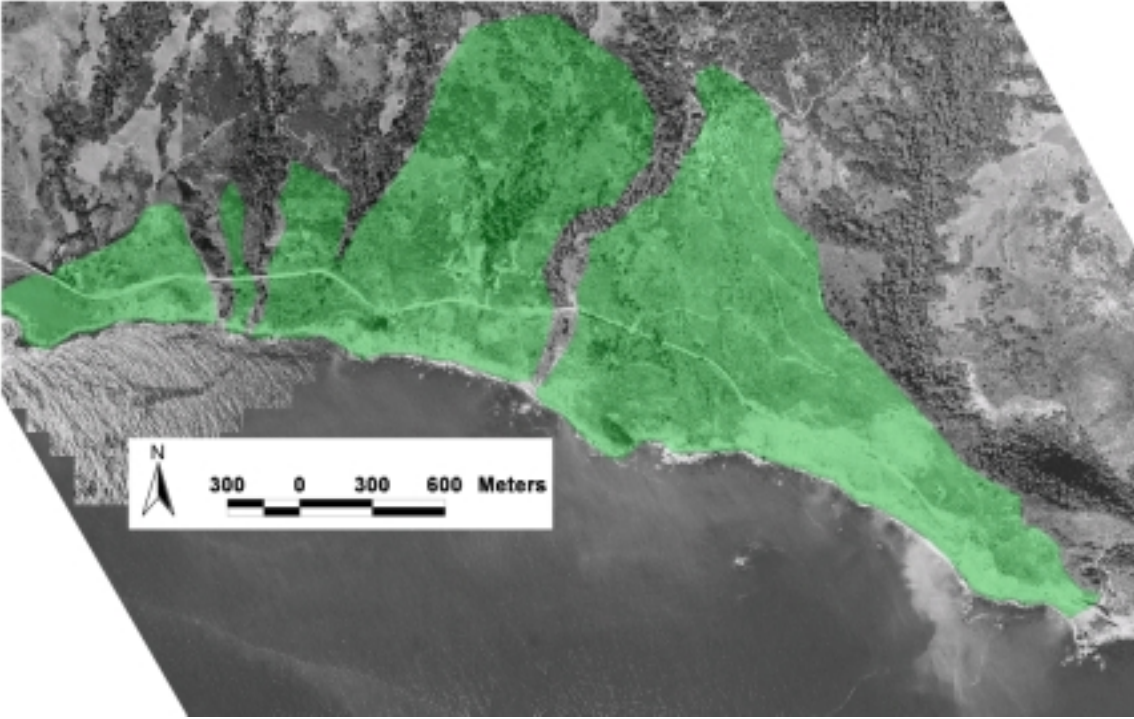


Figure 5: Orthophotomosaic showing delineated polygons within which volumes are calculated for each of the nine sections of coast. This figure shows the polygon for section 6.

elevation that photogrammetric stereo models can confidently derive without significant visual interference from the movement of waves on the water and on the lower part of the beach (Hapke and Richmond, 2000). The volumes from the two dates of photography are then subtracted, and averaged over the polygon areas along each section of coast. This averaging smoothes out the noise generated by localized volume gains in areas where movement on a specific slide has deposited material. Finally, the average value is divided by the total time between the photographs (52 years). This provides an average volumetric loss rate for each section of coastline.

In addition to the rate change determination, orthophotographs and georeferenced images are used in conjunction with the polygons of volumetric change to map locations and spatial distribution of historically active landslides. To supplement the 1942 and 1994 analysis of

landslide distribution, 1929 aerial photographs were obtained for the corridor. Although they are not of sufficient quality to create stereo models, they were georeferenced using the 1994 orthophotographs for control. The distribution of active slopes was then digitized for three dates: pre-highway (1929), immediately post-highway (1942), and present (1994). The active slopes were visually identified by areas of bare earth (not vegetated).

Error Analysis

The total error in the volume calculated for each date includes errors associated with ground control, with the rectification process, as well as the vertical accuracy of the resulting DTM and the accuracy of the images based on the pixel resolution. Ground control errors are related to the accuracy of the original data source for the control. In the case of this study, the x and y positional errors are those associated with the USGS DOQs, and the vertical positional errors are those associated with the enhanced National Elevation Data DEM. The source of the rectification error is the root mean square error (RMSE) determined from the best-fit aerotriangulation transformation in the photogrammetric processing workflow. The rectification error varies from model to model, and is highly dependent on the amount, the distribution, and the quality of the ground control used in the rectification process. Error associated with the vertical accuracy of the DTM is a function of the scale of the stereo photography (Ackerman, 1996), with an additional (unitless) environmental factor, ranging from one to three, to accommodate for nonsystematic errors in the model (Saleh, 2001). For the models developed in this study, an environmental factor of two was applied to the recent (1994) dataset and an environmental factor of three was applied to the historical (1942) data. These errors are suspected to be present based on the extreme relief in the study area, the non-ideal linear distribution of ground control along the coast, and the age of the film and lack of camera calibration data for the historical photography. Finally, the error associated with the pixel resolution of the images is directly related to the resolution at which the photographs are scanned; this is simply the visual limitation of identifying an object (or location) that is smaller in dimension than the pixel size of the digital image. Using standard statistics, the error, or variance, associated with the DTM model for each date is determined by:

$$E_t = [(e_g)^2 + (e_r)^2 + (e_d)^2 + (e_p)^2]^{0.5} \quad (1)$$

where, e_g = ground control error, e_r = rectification error; e_d = dtm error; e_p = pixel resolution; and the subscript t is a given time, or date, from which the data are derived. This error is translated to an uncertainty in volume by assessing the calculated error over the area within which the volume was calculated:

$$\delta_{vt} = (E_t * A)/V_t \quad (2)$$

Where A is the area over which the volume was calculated and V_t is the volume calculated for a particular date. This equation produces a percent volume of the total calculated volume that is within the uncertainty range for that dataset. To determine the total in the volume change calculation, the uncertainties for the two dates are summed:

$$Total\ error = \delta_{v_{1994}} + \delta_{v_{1942}} \quad (3)$$

SEDIMENT YIELD FROM COASTAL LANDSLIDES

The results of the volumetric change analysis are shown in Table 2. The area covered by each section, the shore-parallel length, the total volume loss and the losses per linear extent (sediment yield) of coast are provided for nine sections of coastline along with descriptions of the geologic units from Wills *et al.*, 2001.

The average sediment yield for the Big Sur Highway 1 corridor is approximately $21,000 \pm 1700$ $m^3/km/yr$ ($43,200 \pm 3,500$ $yd^3/mi/yr$) based on the analysis for the completed nine sections. Due to unresolvable non-systematic errors associated with the 1942 photographs, accurate 3D models could not be created for the entire coast. The errors most likely result from distortions in the original film (stretching and warping of old film) and radial distortion associated with older mapping cameras that becomes especially prevalent in areas of extreme relief such as along much of the Big Sur coastline. Since the sediment yield for the entire coastline cannot be determined using the DTM subtraction method described above, the sediment yield is interpolated in areas of missing data. Results of the sediment yield analysis show a strong correlation between the local geology and the sediment delivery rates (Fig. 6); thus rates are estimated by correlating the geology of areas without measured data to areas where the sediment yield was determined.

The sediment yield data vary significantly and range from $1,000 \pm 170 \text{ m}^3/\text{km}/\text{yr}$ ($2,100 \pm 350 \text{ yd}^3/\text{mi}/\text{yr}$) in the northernmost section (section 1, PM 63.1-66.0) to a high of $46,700 \pm 4,800 \text{ m}^3/\text{km}/\text{yr}$ ($97,700 \pm 10,000 \text{ yd}^3/\text{mi}/\text{yr}$) in section 8 (PM 14.0-17.4), north of the town of Gorda. The variation in the delivery rate of material to the base of the slope appears to be closely related to the primary lithology within a given area (Fig. 6). In general, the lowest sediment yield is from the granitic rocks and the resistant sandstone of the Franciscan and the highest yield is in the highly sheared Franciscan mélangé.

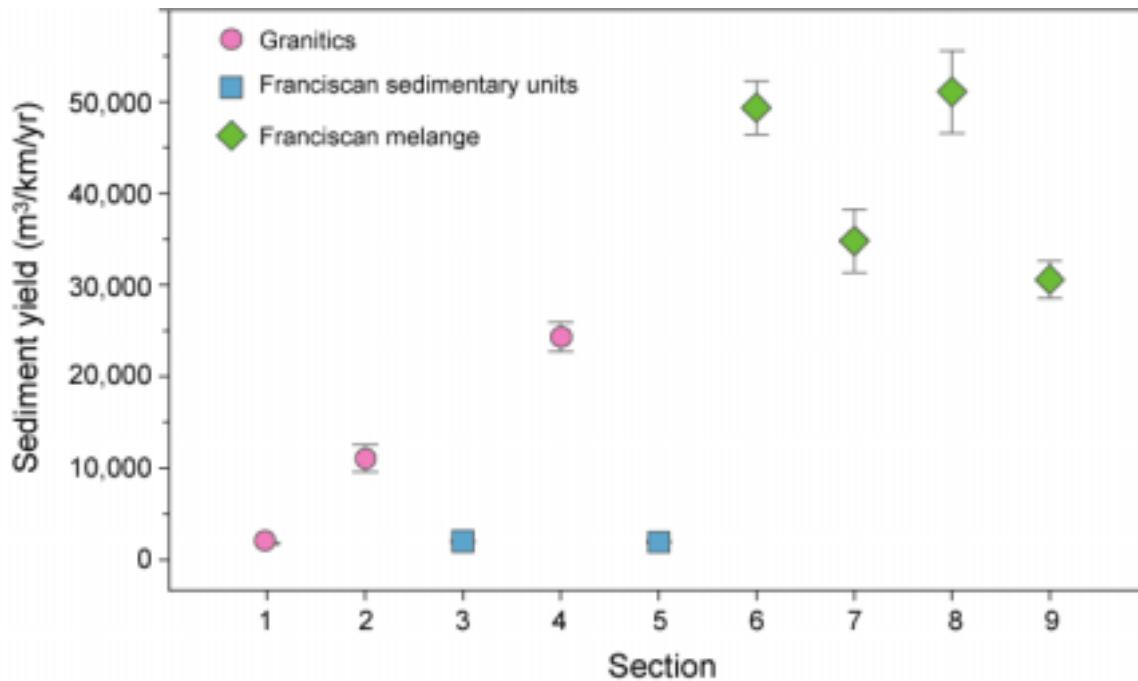


Figure 6: Relationship between lithology and sediment yield for the nine study sections of coastline. The sediment yield within the weak Franciscan mélangé is consistently greater than the yield in the stronger granitics and sedimentary units of the Franciscan complex.

ACTIVE SLOPE DISTRIBUTION

Digital orthoquadrangles from 1994, along with georeferenced imagery of the Big Sur coastline from 1942 and 1929, were used to map the distribution of active slopes for each date. Active slopes were identified by areas showing evidence of recent disturbance such as complete lack of vegetation and clear landslide scars (i.e., headscarps). These areas correspond in part to the

TABLE 2: VOLUME CHANGE AND SEDIMENT YIELD FOR THE NINE STUDY SECTIONS FROM 1942-1994

Section No.	Post mile*	Primary (I) and secondary (II) geologic unit**	Area (km ²)/(mi ²)	Along-coast length (km)/(mi)	Volume change (m ³)/(yd ³)	Sediment yield (m ³ /km/yr)/(yd ³ /mi/yr)
1	63.1 - 66.0	I. Kqd II. Qdf	2.3/ (0.9)	4.5/(2.8)	234,000 ± 39,100/ (306,000 ± 51,100)	1,000 ± 170/ (2,100 ± 350)
2	59.5 – 63.0	I. Kqd, KMct II. Qdf	3.1/ (1.2)	5.5/(3.4)	2,750,000 ± 336,000/ (3,595,000 ± 439,000)	9,600 ± 1,300/ (20,300 ± 2,600)
3	45.6 – 46.6	I. KJf II. Qls	1.3/ (0.5)	2.5/(1.6)	158,000 ± 14,100/ (207,000 ± 18,400)	1,200 ± 100/ (2,500 ± 220)
4	36.8 – 41.5	I. KMct II. Qls	5.0/ (1.9)	7.3/(4.5)	8,328,000 ± 658,000/ (10,886,000 ± 860,000)	21,900 ± 1,700/ (46,400 ± 3,700)
5	26.0 – 29.2	I. KJfmv, KJf II. Qls	3.2/ (1.2)	5.3/(3.3)	313,000 ± 32,000 (409,000 ± 41,800)	1,100 ± 100/ (2,400 ± 250)
6	21.3 – 24.1	I. KJfmv II. Qls	3.5/ (1.4)	5.0/(3.1)	11,700,000 ± 842,000/ (15,300,000 ± 1,100,000)	45,100 ± 3,300/ (94,900 ± 6,800)
7	19.4 – 21.2	I. KJfmv, KJf II. Qls	1.2/ (0.5)	3.0/(1.9)	4,936,000 ± 578,000/ (6,450,000 ± 756,000)	31,600 ± 3,700/ (65,300 ± 7600)
8	14.0 – 17.4	I. KJfmv, KJfgw, KJfs II. Qdf/Qom/Qls	4.7/ (1.8)	8.0/(5.0)	19,400,000 ± 1,979,000 (25,400,000 ± 2,590,000)	46,700 ± 4,800/ (97,700 ± 10,000)
9	73.0 (SLO)– 3.5 (MON)	I. KJfgw, KJfs II. Qls	3.0/ (1.2)	5.0/(3.1)	7,100,000 ± 540,000 (9,280,000 ± 706,000)	27,700 ± 2,100/ (57,600 ± 4,300)

*All post miles are in Monterey County unless otherwise denoted.

**Refer to Table 1 for descriptions of geology.

historic landslides mapped by Wills *et al.* (2001). However, individual active slope delineations do not necessarily define the entire extent of a particular landslide, rather only that portion of a landslide or cliff face that was active at the time the photographs were taken. The linear distribution of active slopes for each year is shown on Maps 1-3, as strips parallel to the coastline. Each of the three active slope strips represents the coast-parallel extent of areas where subaerial active slopes were identified for a particular date of aerial photography.

From the temporal and spatial distribution of landslides, it is evident that much of this region was undergoing active slope failure during the construction of coastal Highway 1 in 1929, and in many places the slopes were again active in both 1942 and 1994. The most active

area for all time periods is in the southernmost section (Map 1) that corresponds well to the weaker rocks of the Franciscan Complex. The rocks within this section are predominantly highly sheared Franciscan *mélange* and are substantially weaker than the granitic rocks and the less sheared Franciscan-Complex rocks to the north (Map 3).

APPLICATIONS AND LIMITATIONS

The purpose of this study is to estimate the long-term sediment input to the MBNMS along the Big Sur coastline directly from coastal landslides. In addition, the spatial and temporal distribution of active slopes from three dates of photographs was delineated and included on the maps. The volumetric analysis was designed to determine, within an order of magnitude, the amount sediment that has been input to the nearshore environment over a 52-year period from 1942 to 1994. The 1942 photography was the oldest photography available that met the requirements of the technique: stereo coverage, coast-parallel flight line, and a scale that reasonably covers the approximately 120 km (75 mi) of coastline. Since both data sets post-date the construction of Highway 1 through the region, there is no way to resolve the deviation from the natural input that can be attributed solely to highway construction or management practices. There is no dataset currently available that would provide the information to completely separate the pre-highway sediment input from the post-highway input.

The sediment yield data presented in this report are expressed as yearly averages. While average values are often very useful for long-term management planning, the actual landslide processes are highly episodic, and failure on one large landslide may account for most of the volume loss in any given area. In addition, the movement on a single slide does not necessarily result in immediate input to the nearshore system. Instead, the slides often creep over several weeks or a winter season or even over a several year time period. Ultimately, large masses of broken material are deposited near the base of the slope where continued sliding and dispersion by waves eventually results in the removal of the material.

The technique used in this study could not be applied to the entire length of the Big Sur coast due to poor data quality of many of the historical photographs. As a result, it was necessary to interpolate the sediment yields in these areas relating the geology to the quantified sediment

yields. Although there is good correlation between the rock type and the estimated sediment yield, the interpolated data should be used with caution, as the geology varies dramatically along-coast, even within the same general lithology.

For the active slope distribution mapping, an additional data set (1929 photographs) was used in order to extend the overall time span of the analysis. The distribution maps show where the areas of active slopes are concentrated, both spatially and temporally. This provides a snapshot of the active portions of the coastal slope at the time the photographs were taken, and information on how the areas of active slopes may have spatially migrated through time. Limitations of the active slope distribution mapping include problems with mapping the active slopes with photographs of different scales, as well as issues with the data quality of the older photographs. For example, the 1929 photographs have the largest scale of the three datasets, and therefore feature details should be more resolvable than on the smaller scale photographs. However, because of the age of the original film, and the quality of the aerial camera with which the photographs were collected (compared to modern mapping cameras), features may be more difficult to identify than on the better quality 1994 photographs.

SUMMARY

Coastal Highway 1 in Monterey and San Luis Obispo counties runs along the rugged and remote Big Sur coastline at the base of the Santa Lucia Range. The region is tectonically active and continued uplift has created one of the steepest coastal slopes in the contiguous U.S. The steep slopes are, along much of this coastline, formed in the very weak *mélange* of the Franciscan formation. In addition, this region experiences both high amounts of precipitation and high wave energy in the winter months. All these factors combine to produce an area of chronic landslides that regularly block, undermine or damage Highway 1. Large volumes of material often must be removed from the highway after a landslide and additional material is frequently generated when the slopes are stabilized to prevent further damage to the highway. The water extending from the base of the slopes along the entire Big Sur coast is part of the Monterey Bay National Marine Sanctuary and it is against federal regulations to dump or dispose of any material into a national marine sanctuary due to the possibility of negatively impacting the nearshore habitat.

The aim of this study is to provide background information on the volumes of material that historically enter the MBNMS along the Big Sur coast directly from coastal landslides, and to map both the spatial and temporal distribution of areas of active input. Using digital stereo photogrammetry, terrain models were created for 2 dates spanning a 52-year time period. The volume change could then be calculated by subtracting the terrain models. A sediment yield (volume loss per linear extent of coast per year) was derived using this method for nine sections of coastline. The average sediment yield was found to be $21,000 \pm 1,700 \text{ m}^3/\text{km}/\text{yr}$ ($43,200 \pm 3,500 \text{ yd}^3/\text{mi}/\text{yr}$). The largest inputs are within the weakest materials that are concentrated in the southern portion of the area, while the lowest input rates were found to be within the stronger rocks, located primarily in the northern portion of the Big Sur coast. In the areas where the sediment yield could not be directly calculated, the yields were interpolated by correlating with the geology in areas where sediment yields were determined. The interpolated areas are shown as dashed lines on the maps.

In addition to the sediment yield data for the coast, the maps also show the distribution of active slopes along the coast. Using georeferenced photography from 1929 (which pre-dates the construction of the road) along with the photography from 1942 and 1994 used in the volumetric analysis, locations of active slopes were digitized in a GIS.

In general, the maps show that both the locations of the active slopes as identified in the three dates of photographs, and the higher sediment yields occur in the weak rocks of the Franciscan Complex. These areas also correspond to areas of historic and dormant landslides as mapped by Wills *et al.* (2001). This suggests that the locations and rates of material influx to the nearshore zone is not a recent phenomenon, rather has been occurring for hundreds or even thousands of years. The technique developed for this study of determining the sediment yield from the coastal landslides has provided Caltrans' Coast Highway Management Plan with background data regarding the average volumetric input along the coast.

ACKNOWLEDGEMENTS

We extend thanks to engineering geologist John Duffy of Caltrans District 5 for sharing his extensive knowledge of geology and landslide processes along the Big Sur coast, and Aileen Loe of Caltrans District 5 for all her coordination efforts and for making this research project possible. Laurie McBean of PCI Geomatics provided valuable technical support. We also benefited greatly from conversations with Lee Otter, Chris Wills, Mark Reid, Kevin Schmidt and Lew Rosenberg regarding the geology of the Big Sur coast and landslide processes. The Caltrans Big Sur Coastal Highway Management Plan and the USGS Coastal and Marine Geology Program funded this research.

REFERENCES

- Ackerman, F., 1996, Techniques and strategies for DEM generation, *in* Greve, C., ed., Digital Photogrammetry: An Addendum to the Manual of Photogrammetry: Bethesda, MD, American Society for Photogrammetry and Remote Sensing, p. 135-141.
- Bailey, E.H., Irwin, W.P., and Jones, D.L., 1964, Franciscan and related rocks and their significance in the geology of western California: California Division of Mines and Geology Bulletin 183, XX p.
- Blake, M.C., Jr., Jayko, A.S., McLaughlin, R.J., and Underwood, M.B., 1988, Metamorphism and tectonic evolution of the Franciscan Complex, northern California, *in* Ernst, W.G., ed., Metamorphism and crustal evolution of the western United States; Rubey Volume 7: Englewood Cliffs, New Jersey, Prentice-Hall, p. 1035-1060.
- California Coastal Commission, 1987, California Coastal Resource Guide, University of California Press.
- Cleveland, G.B. 1975, Landsliding in Marine Terrace Terrain, California: California Division of Mines and Geology, Special Report 119.
- Coastal Data Information Program, 2002, U.S. Army Corps of Engineers/CA Dept. of Boating and Waterways/Scripps Inst. of Oceanography, electronic data (<http://cdip.ucsd.edu>).
- Compton, R.R., 1966, Granitic and metamorphic rocks of the Salinian block, California Coast Ranges: California Division of Mines and Geology Bulletin 190, p. 277-287.

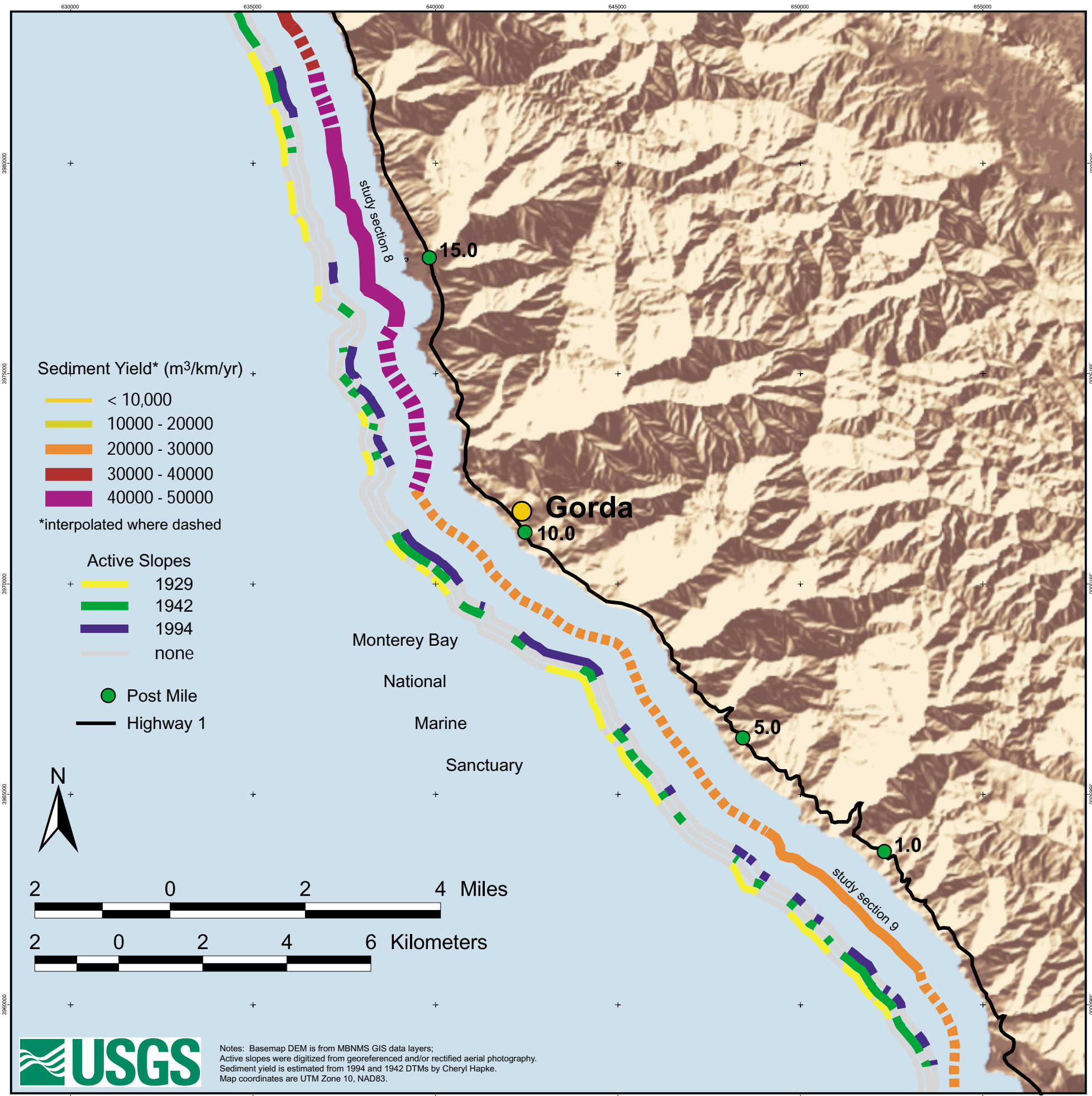
- Dibblee, T.W., Jr. 1974, Geologic Maps of the Monterey, Salinas, Gonzales, Point Sur, Jamesburg, Soledad and Junipero Serra quadrangles, Monterey County, California: U.S. Geological Survey Open-File Report 74-1021, scale 1:62,500, 1 sheet.
- Engellenner, J. 1984, Party reopens scenic highway: Santa Cruz Sentinel, April 12, 1984.
- Falkner, E., 1995, Aerial Mapping Methods and Applications: Boca Raton, FL, Lewis Publishers, XX p.
- Gilliam, H., 1962, Weather of the San Francisco Bay region, Natural History Guide 6: Berkeley, University of California Press.
- Hall, C.A., Jr., 1991, Geology of the Point Sur-Lopez Point region, Coast Ranges, California: A part of the Southern California allochthon: Geological Society of America Special Paper 266, 40 p.
- Hapke, C. and Richmond, B., 2000, Monitoring beach morphology changes using small-format aerial photography and digital softcopy photogrammetry: Environmental Geosciences, v. 7, n. 1, p. 32-37.
- Henson, P., and Usner, D.J., 1993, The Natural History of Big Sur: Berkeley, University of California Press, 416 p.
- James, E.W., and Mattinson, J.M., Metamorphic history of the Salinian block: An isotopic reconnaissance, *in* Ernst, W.G., ed., Metamorphism and crustal evolution of the western United States; Rubey Volume 7, Englewood Cliffs, New Jersey, Prentice-Hall, p.938-952.
- Komar, P.D., 1998, Beach Processes and Sedimentation: Upper Saddle River, New Jersey, Prentice Hall, 544 p.
- Maune, D.F., Kopp, S.M., Crawford, C.A., and Zervas, C.E., 2001, Introduction: Digital Elevation models, *in* Maune, D.F., ed., Digital Elevation Model Technologies and Applications: The DEM Users Manual: Bethesda, Maryland, American Society of Photogrammetry and Remote Sensing, p. 1-34.
- NOAA, 2002, National Marine Sanctuary Regulations.
<http://www.sanctuaries.nos.noaa.gov/natprogram/npregulation/npregulation.html>.
- Page, B.M., 1982, Migration of Salinian composite block, California, and disappearance of fragments: American Journal of Science, v. 282, p. 1694-1734.
- Ross, D.C., 1976, Reconnaissance geologic map of the pre-Cenozoic basement rocks, northern Santa Lucia Range, Monterey County, California: U.S. Geological Survey Miscellaneous Field Studies Map MF-750, 1 sheet.

- Saleh, R.A., 2001, A Handle on the accuracy of imagery-based digital elevation data in a softcopy environment, Workshop #2, Measuring the Earth – Digital Elevation Technologies and Applications, MAPPS-ASPRS Conference, St. Petersburg, FL, 45 p.
- Slama, C., ed., 1980, Manual of Photogrammetry: Falls Church, VA, American Society of Photogrammetry, 1056 p.
- Wills, C.J., Manson, M.W., Brown, K.D. Davenport, C.W., and Domrose, C.J., 2001, Landslides in the Highway 1 Corridor: Geology and Slope Stability Along the Big Sur Coast, Report to the Coast Highway Management Plan Caltrans District 5, 29 p.
- Wolf, P.R. and Dewitt, B.A., 2000, Elements of Photogrammetry with Applications in GIS: Boston, McGraw Hill, 3rd ed., 608 p.
- Works, B., 1984, Landslide on State Highway 1: California Geology, p.130-131.

Landslide Sediment Yield and Active Slope Distribution: Big Sur Coastline, California

C. Hapke, K. Dallas and K. Green, U.S.G.S. Pacific Science Center

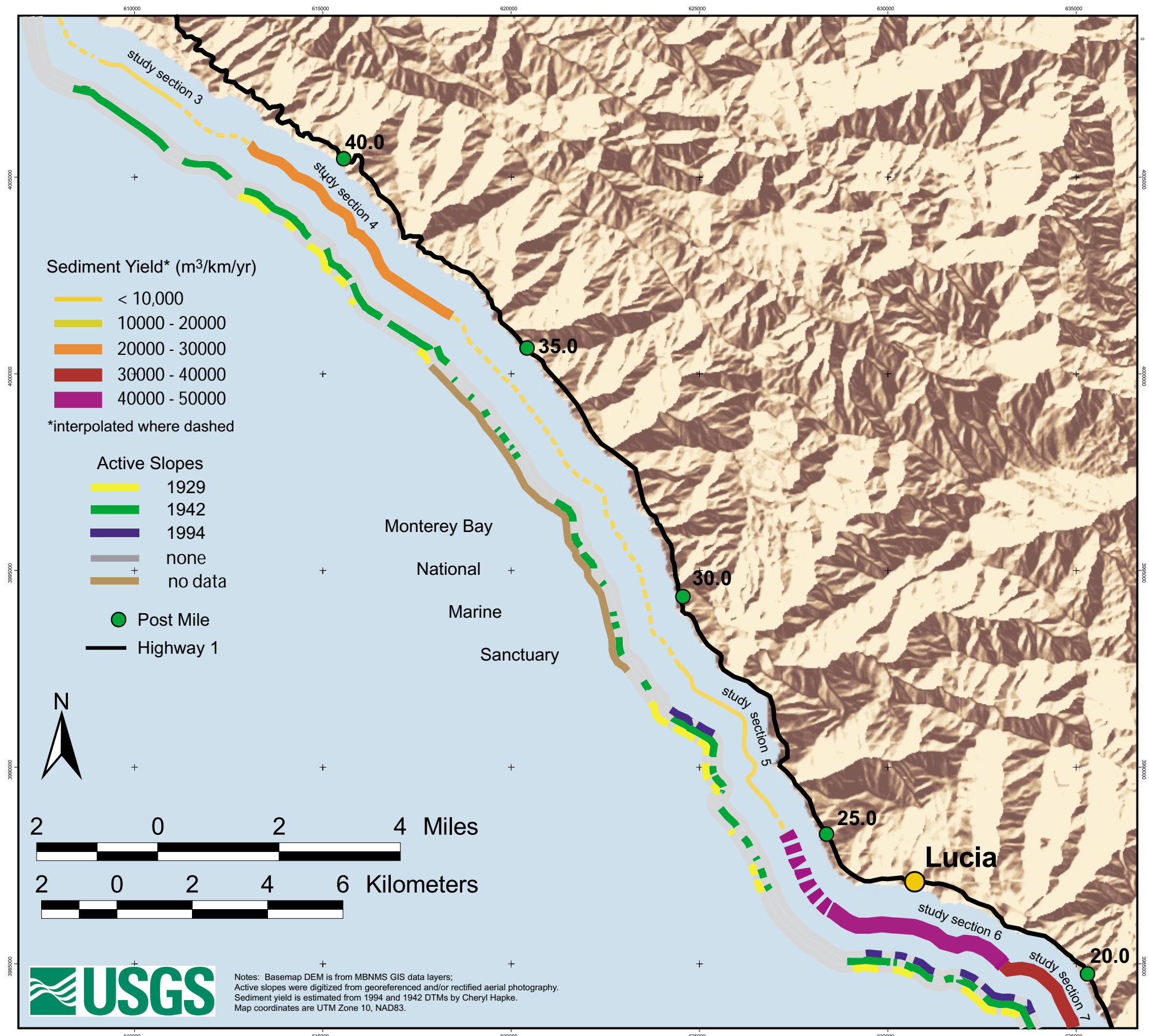
MAP 1 - Southern Section



Landslide Sediment Yield and Active Slope Distribution: Big Sur Coastline, California

C. Hapke, K. Dallas and K. Green, U.S.G.S. Pacific Science Center

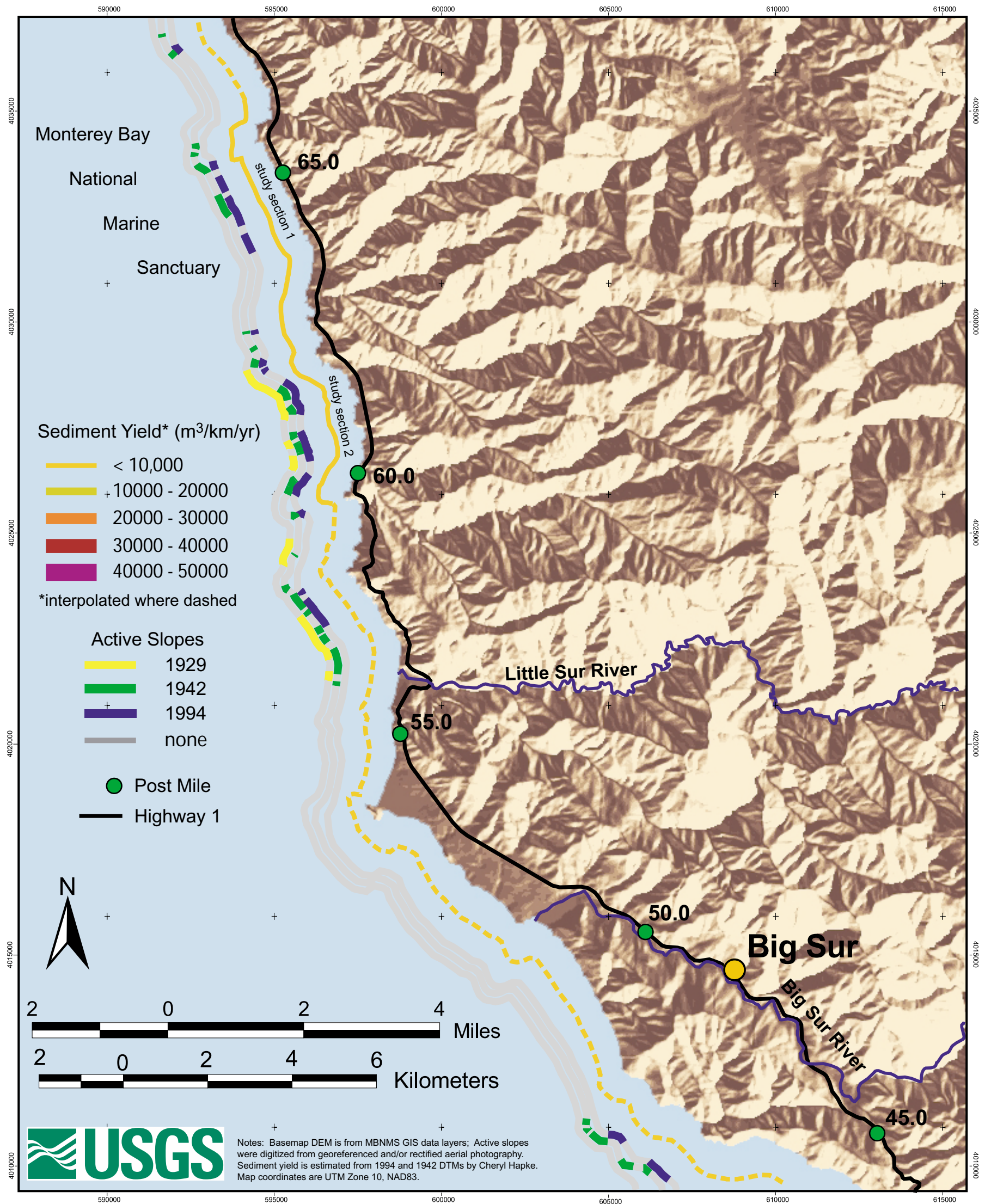
MAP 2 - Central Section



Landslide Sediment Yield and Active Slope Distribution: Big Sur Coastline, California

C. Hapke, K. Dallas and K. Green, U.S.G.S. Pacific Science Center

MAP 3 - Northern Section





COASTAL CLIFF EROSION RATES BIG SUR, CALIFORNIA

**A Report of Findings for the
COASTAL HIGHWAY MANAGEMENT PLAN
CALIFORNIA DEPARTMENT OF TRANSPORTATION, DISTRICT 5**

**Prepared by
C. Hapke¹
K. Green²**

**¹U.S. GEOLOGICAL SURVEY, PACIFIC SCIENCE CENTER
and
²UNIVERSITY OF CALIFORNIA, SANTA CRUZ**

May 2003



EXECUTIVE SUMMARY

Along the Big Sur coastline, the Santa Lucia Mountains descend steeply into the Pacific Ocean. Coast Highway 1 runs along the edge of the coastal slope, and the waters adjacent to the Big Sur coastline are within the Monterey Bay National Marine Sanctuary (MBNMS). Highway 1 is frequently undermined or damaged by the retreat of the coastal cliffs in this area, which occur near the base of the coastal slope. Little is known about the rate at which the cliffs retreat in this area. Upon failure, cliff material provides protection from waves at the base of the slope, and sediment entering the water provides nutrients and material for various nearshore habitats.

The focus of this analysis is to provide coastal cliff retreat rates for the Big Sur coastline. The purpose is to provide background data for the Coast Highway Management Program and to advance the fundamental understanding of coastal cliff retreat along this stretch of coastline.

The cliff retreat rates are derived by applying digital photogrammetric and GIS techniques to create 3D stereo models of nine discontinuous sections of the coast from 2 dates of vertical aerial photography. The cliffs are digitized directly from the models while viewing in stereo, and a software program is used to generate transects along which the retreat rates are calculated.

In general, the areas with low retreat rates are in the stronger granitic rocks that are concentrated along the northern portion of the Big Sur area. The highest rates are within the Franciscan Complex rocks that dominate in the central and southern portions of the coastline. The rates range from 12 ± 5 cm/yr (5 ± 2 in/yr) to a high of 25 ± 5 cm/yr (10 ± 2 in/yr).

INTRODUCTION

The purpose of this study is to quantify the long-term cliff erosion rates along the Big Sur coast. Based on data availability, erosion rate calculations are restricted to the geographic limits of the coast that correspond to the nine study sections along which sediment yield was previously determined (Fig. 1)(Hapke et al., 2003). This study was undertaken as a direct result of the identification that there was a fundamental lack of data on the rates at which the coastal cliffs along Highway 1 are retreating landward. As a result, Caltrans committed resources through the CHMP to support the necessary research activities related to filling data gaps.

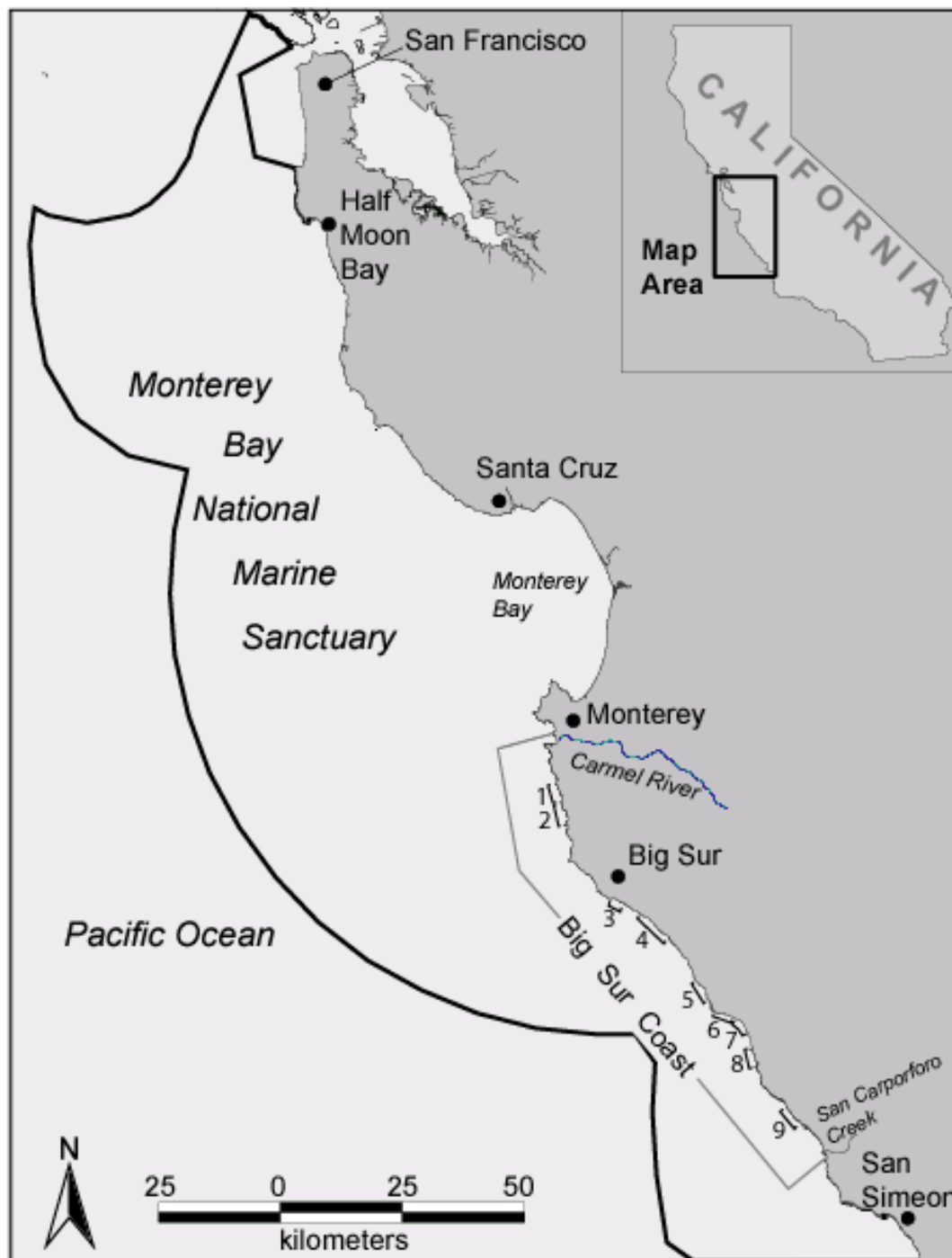


Figure 1: Map showing location of the MBNMS and the Big Sur coast in central California. The numbers 1-9 shown on the map correspond to the specific study sections.

The erosion reference feature is well defined in some areas as a very sharp cliff edge (Fig. 2, location A), such as where marine terraces are present. In other parts of the coastline, the cliff edge is very poorly defined. In these areas the erosion reference feature is actually the edge of the man-made road grade in those areas where the basal portion of the slope is visibly active from the slope base to the road grade (Fig. 2, location B). In other areas the erosion reference feature is the active lower portion of the slope where the slope is not visibly active to the road grade (Fig. 2, location C). To avoid confusion in terminology, “cliff retreat rate” will be used to refer to the landward retreat of all of these features.



Figure 2: Oblique photo of the Big Sur coast near Hurricane Point. The red line shows the feature digitized as the cliff edge. The letters A, B, and C represent different morphologies of the cliff edge.

METHODS

The primary tools used in this analysis are digital photogrammetry and GIS. Digital photogrammetry is used to process the historical (1942) and recent (1994) vertical aerial photographs to generate 3D stereo models. The cliff edges are digitized directly from the models while viewing in stereo to assure the actual break in slope is digitized as the erosion reference feature (cliff edge). The cliff edges are then brought into a GIS where a shore-parallel baseline is generated. The baseline can follow the shape of the coast, or it may be a straight line with the same azimuth as the average orientation of the coastline. For the average rates generated for each section (Table 1), a coast-following baseline was used for greater accuracy. However, for purposes of clarity on the maps (Appendix 1), a straight baseline was used. Once the baseline is established, orthogonal transects extending from the baseline to the coast are generated using the Digital Shoreline Assessment System (DSAS; Thieler et al., 2003). The spacing of the transects for the average erosion rate calculations for each section is 15 m, and for the maps, the spacing is 25 m. DSAS is then used to calculate the positional difference between the 2 cliff edges along each transect to establish cliff edge retreat rates.

COASTAL CLIFF RETREAT

The results of the cliff retreat analysis are shown in Table 1. The shore-parallel length for each section and the average cliff retreat rates are provided for nine sections of coastline along with descriptions of the geologic units from Wills *et al.*, 2001.

The average cliff retreat rate for the Big Sur Highway 1 corridor is approximately 18 ± 6 cm/yr (7 ± 2 in/yr) based on the analysis for the completed nine sections. The rates vary significantly and range from 12 ± 5 cm/yr (5 ± 2 in/yr) in the northernmost section (section 1, PM 63.1-66.0) to a high of 25 ± 5 cm/yr (8 ± 2 in/yr) in section 3 (PM 45.6-46.6), near the town of Big Sur.

TABLE 1: COASTAL CLIFF RETREAT RATES FOR THE NINE STUDY SECTIONS FROM 1942-1994

Section No.	Post mile*	Primary (I) and secondary (II) geologic unit**	Along-coast length km/(mi)	Retreat rate cm/yr (in/yr)
1	63.1 - 66.0	I. Kqd II. Qdf	4.5/(2.8)	12 ± 5 (5 ± 2)
2	59.5 – 63.0	I. Kqd, KMct II. Qdf	5.5/(3.4)	12 ± 5 (5 ± 2)
3	45.6 – 46.6	I. KJf II. Qls	2.5/(1.6)	25 ± 5 (10 ± 2)
4	36.8 – 41.5	I. KMct II. Qls	7.3/(4.5)	22 ± 5 (9 ± 2)
5	26.0 – 29.2	I. KJfmv, KJf II. Qls	5.3/(3.3)	21 ± 5 (8 ± 2)
6	21.3 – 24.1	I. KJfmv II. Qls	5.0/(3.1)	17 ± 5 (7 ± 2)
7	19.4 – 21.2	I. KJfmv, KJf II. Qls	3.0/(1.9)	17 ± 5 (7 ± 2)
8	14.0 – 17.4	I. KJfmv, KJfgw, KJfs II. Qdf/Qom/Qls	8.0/(5.0)	20 ± 8 (8 ± 3)
9	73.0 (SLO)– 3.5 (MON)	I. KJfgw, KJfs II. Qls	5.0/(3.1)	20 ± 6 (8 ± 2)

*All post miles are in Monterey County unless otherwise denoted.

**Refer to Wills *et al.*, 2001 for descriptions of geology.

The cliff retreat rates presented in this report are expressed as yearly averages. While average values are often very useful for long-term management planning, the actual processes of cliff retreat are highly episodic wherein a large retreat event during a series of storms may account for most of the volume loss in any given area.

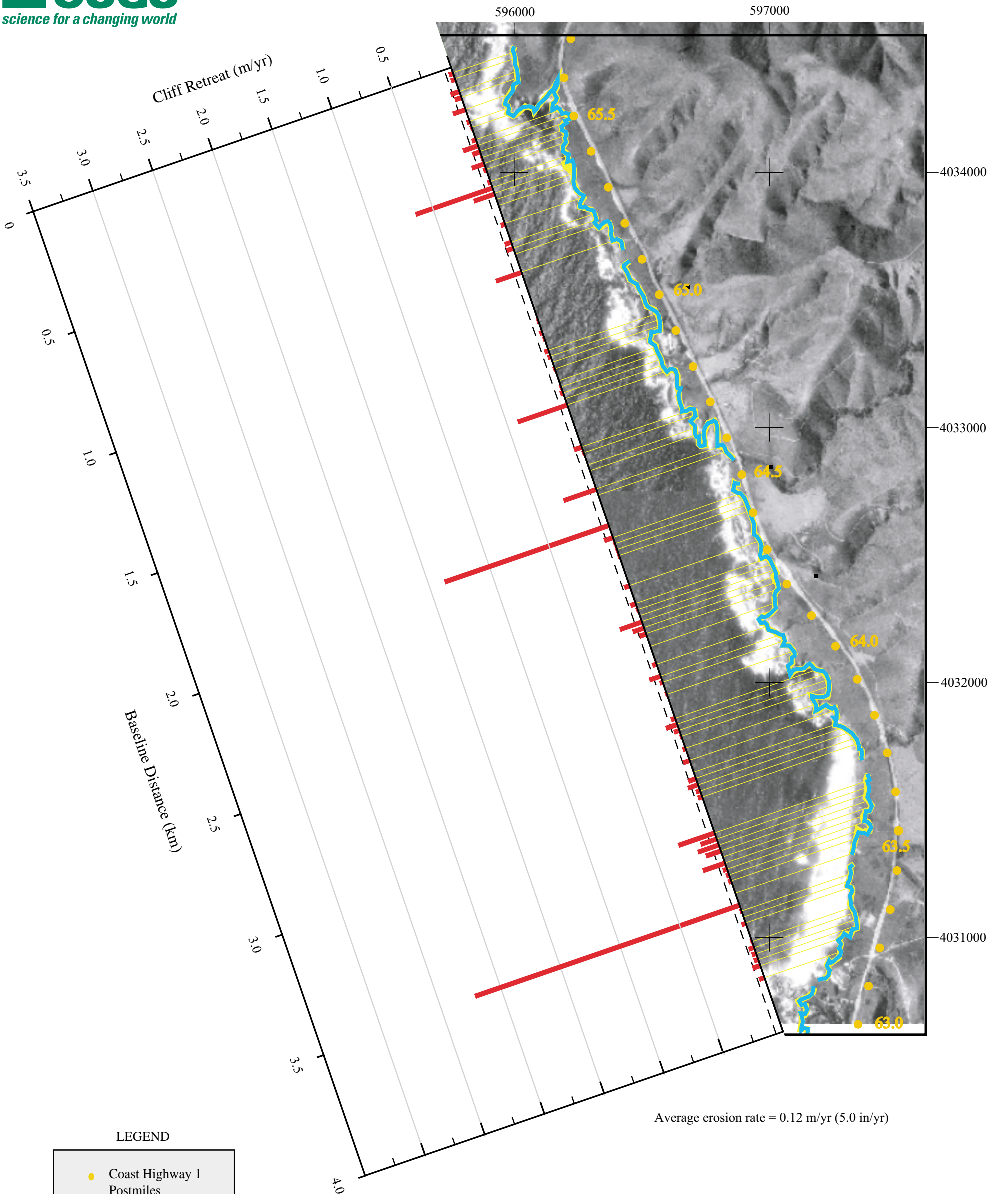
SUMMARY

Coastal Highway 1 in Monterey and San Luis Obispo counties is regularly subjected to damage from coastal cliff retreat, as the steep slopes experience both high amounts of precipitation and high wave energy in the winter months. This study provides coastal cliff erosion rates along nine discontinuous sections of the Big Sur coast. Stereo models from a previous study (Hapke *et al.*, 2003) were used to digitize cliff edges, and the retreat rates were calculated for a 52-year time period. The average cliff retreat rate was found to be 18 ± 6 cm/yr (7 ± 2 in/yr). The lowest

retreat rates (12 ± 5 cm/yr; 5 ± 2 in/yr) were found to be within the stronger granitic rocks, located primarily in the northern portion (sections 1 and 2) of the Big Sur coast. The highest rate (25 ± 5 cm/yr; 10 ± 2 in/yr) is along the coast near Wreck Beach where it appears a large promontory on the slope completely eroded back or collapsed during the time period of the analysis. This section of coast is the closest to the town of Big Sur, in an area where Highway 1 is significantly inland from the coast.

REFERENCES

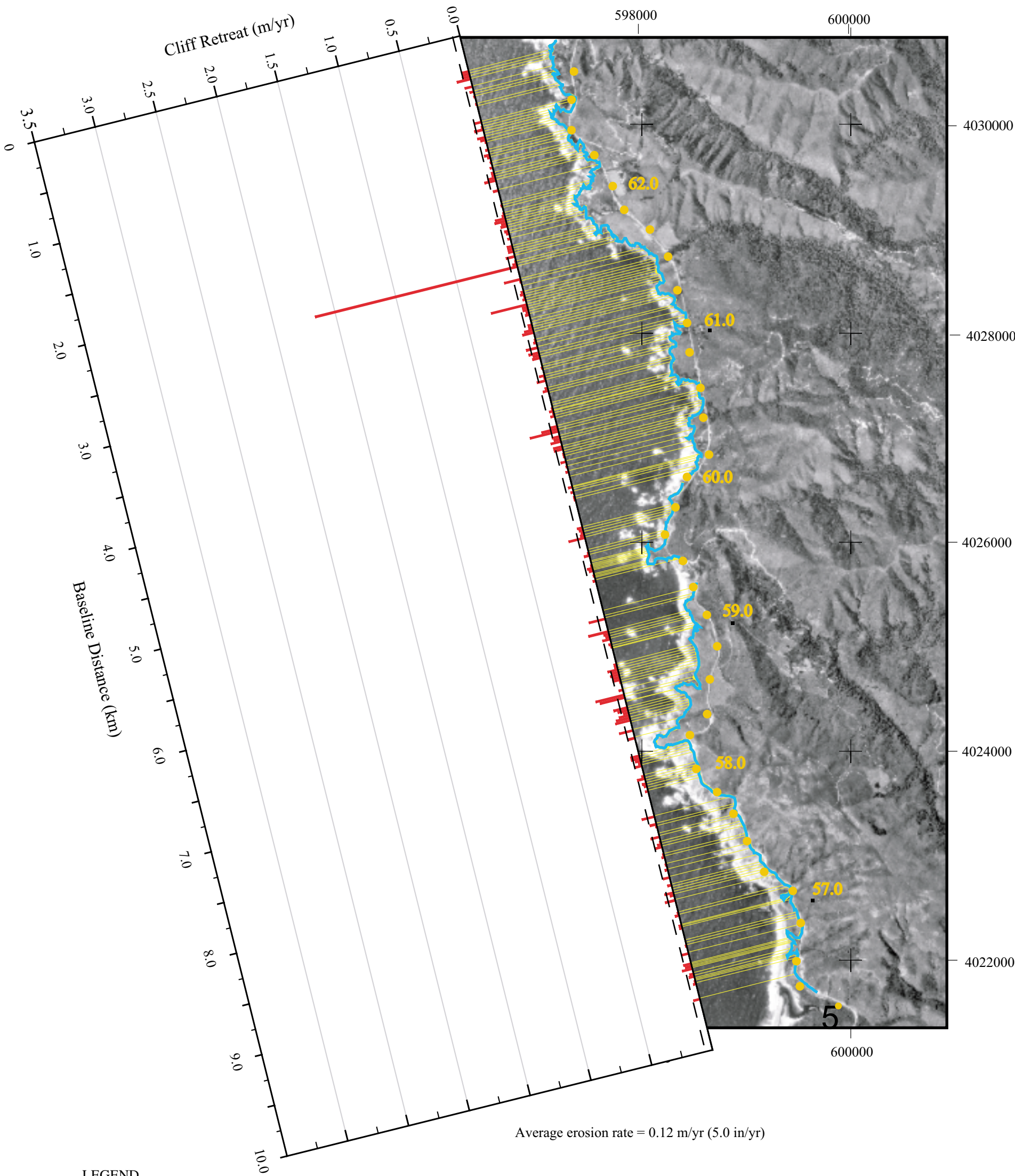
- Hapke, C., Green, K., and Dallas, K., 2003, Estimated sediment yield from coastal landslides and active slope distribution, Big Sur, California, Report to the Coast Highway Management Plan Caltrans District 5, 26 p.
- Thieler, E. R., Martin, D., and Ergul, A., 2003, The Digital Shoreline Analysis System, version 2.0: Shoreline change measurement software extension for ArcView. USGS Open-File Report 03-076.
- Wills, C.J., Manson, M.W., Brown, K.D. Davenport, C.W., and Domrose, C.J., 2001, Landslides in the Highway 1 Corridor: Geology and Slope Stability Along the Big Sur Coast, Report to the Coast Highway Management Plan Caltrans District 5, 29 p.



Cliff Erosion Rates, Big Sur, CA, Section 1 (PM 63.0-66.0)

by
Cheryl Hapke and Krystal Green

Orthophotograph from USGS DOQ, UTM Zone 10, NAD83. Transects and erosion rates were generated using the Digital Shoreline Analysis System (Thieler, E. R., Martin, D., and Ergul, A., 2003. The Digital Shoreline Analysis System, version 2.0: Shoreline change measurement software extension for ArcView. USGS Open-File Report 03-076.). Cliff edges were derived from 1994 and 1942 topographic models generated from stereo aerial photographs by Cheryl Hapke.



LEGEND

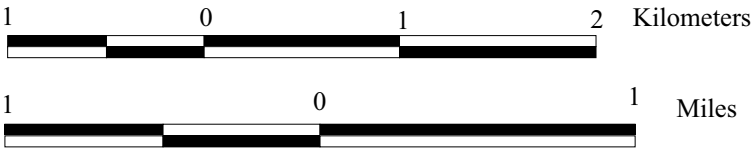
Coast Highway 1 Postmiles

1994 Cliff Edge

1942 Cliff Edge

Transects

error line



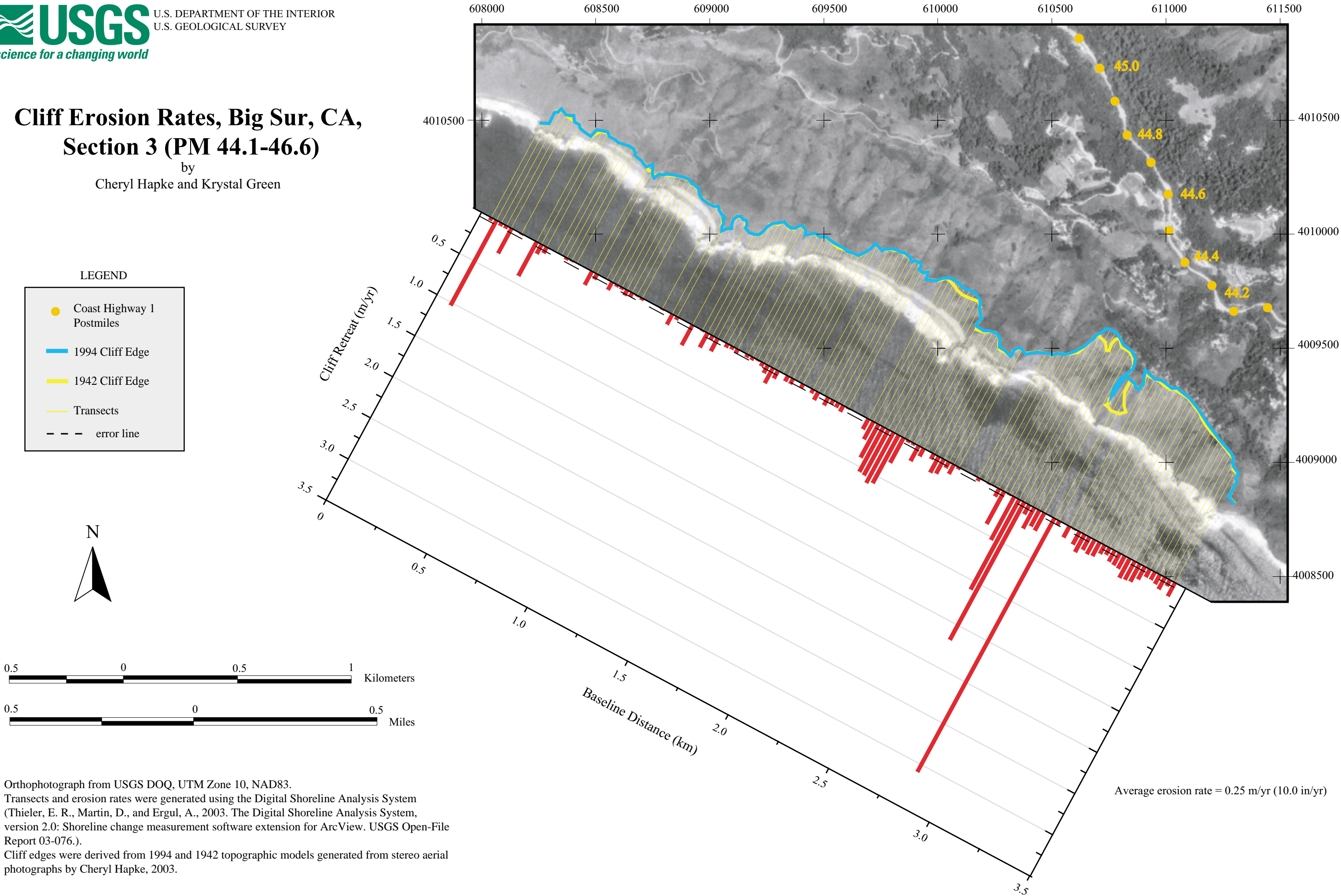
Cliff Erosion Rates, Big Sur, CA, Section 2 (PM 56.2-63.0)

by
Cheryl Hapke and Krystal Green

Orthophotograph from USGS DOQ, UTM Zone 10, NAD83.
Transects and erosion rates were generated using the Digital Shoreline Analysis System (Thieler, E. R., Martin, D., and Ergul, A., 2003. The Digital Shoreline Analysis System, version 2.0: Shoreline change measurement software extension for ArcView. USGS Open-File Report 03-076.).
Cliff edges were derived from 1994 and 1942 topographic models generated from stereo aerial photographs by Cheryl Hapke.

Cliff Erosion Rates, Big Sur, CA, Section 3 (PM 44.1-46.6)

by
Cheryl Hapke and Krystal Green



Cliff Erosion Rates, Big Sur, CA, Section 4 (PM 35.0-41.6)

by
Cheryl Hapke and Krystal Green

LEGEND

- Coast Highway 1 Postmiles
- 1994 Cliff Edge
- 1942 Cliff Edge
- Transects
- - - error line



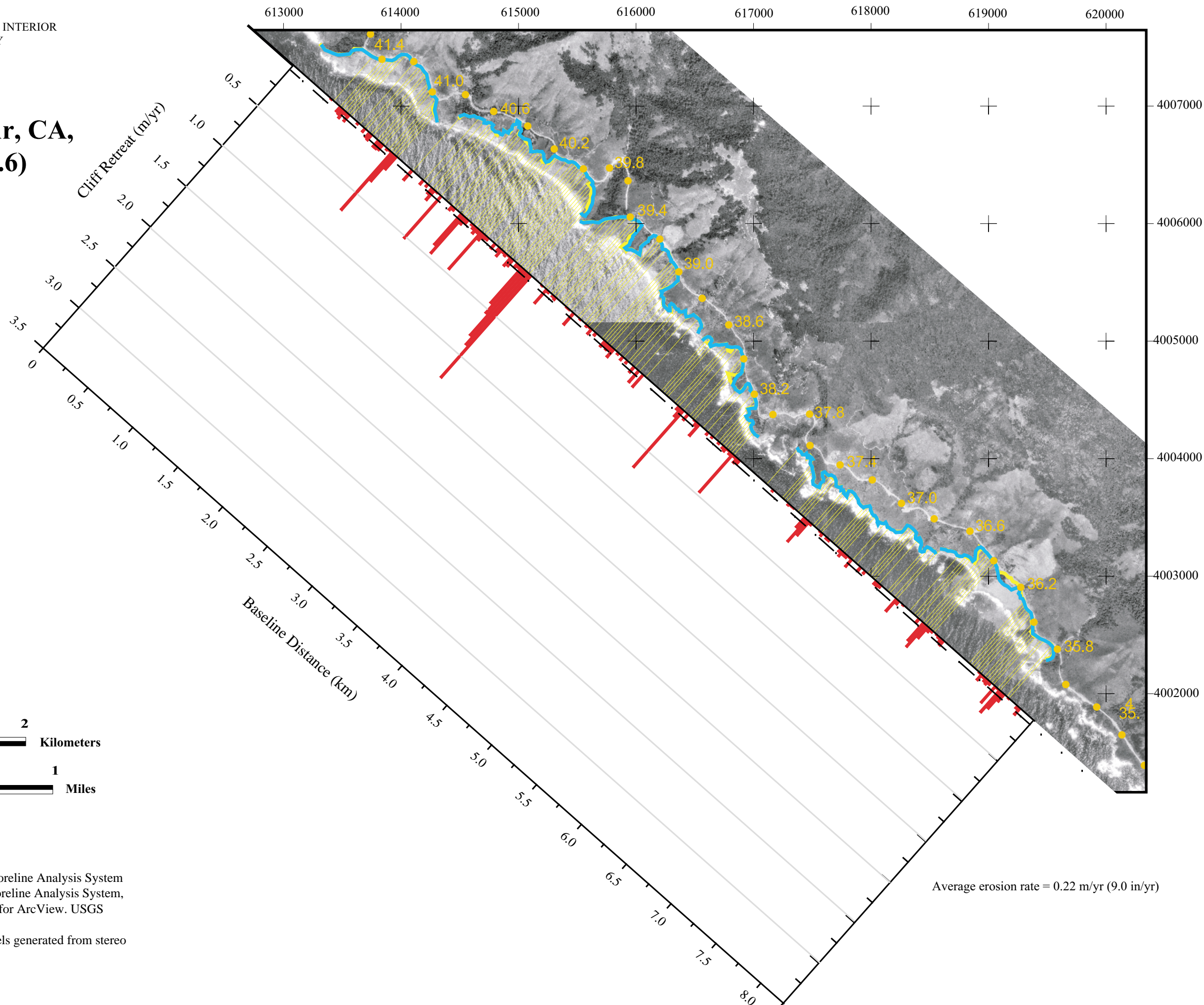
1 0 1 2
Kilometers

1 0 1
Miles

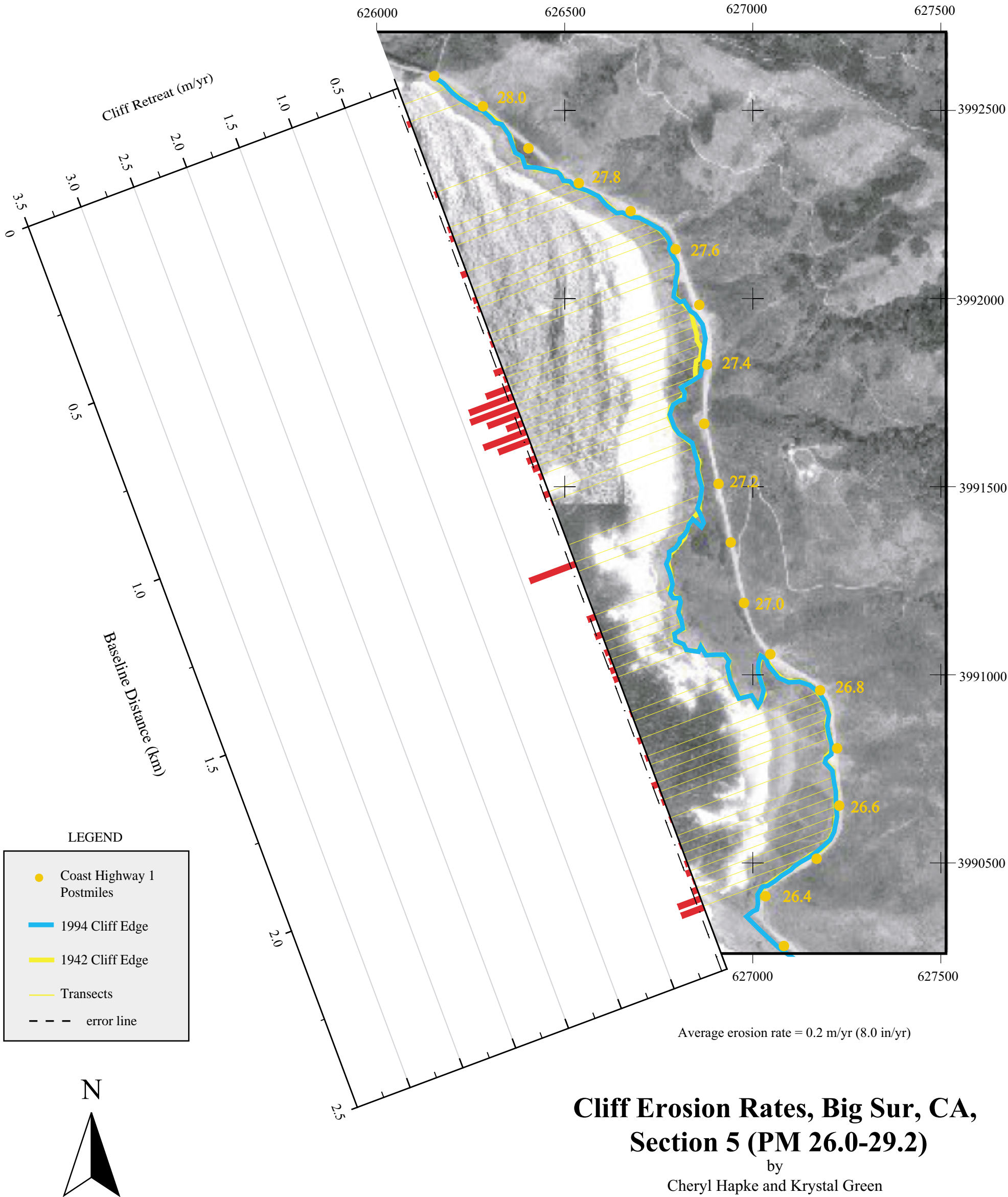
Orthophotograph from USGS DOQ, UTM Zone 10, NAD83.

Transects and erosion rates were generated using the Digital Shoreline Analysis System (Thieler, E. R., Martin, D., and Ergul, A., 2003. The Digital Shoreline Analysis System, version 2.0: Shoreline change measurement software extension for ArcView. USGS Open-File Report 03-076.).

Cliff edges were derived from 1994 and 1942 topographic models generated from stereo aerial photographs by Cheryl Hapke, 2003.



Average erosion rate = 0.22 m/yr (9.0 in/yr)



Orthophotograph from USGS DOQ, UTM Zone 10, NAD83.
Transects and erosion rates were generated using the Digital Shoreline Analysis System (Thieler, E. R., Martin, D., and Ergul, A., 2003. The Digital Shoreline Analysis System, version 2.0: Shoreline change measurement software extension for ArcView. USGS Open-File Report 03-076.).
Cliff edges were derived from 1994 and 1942 topographic models generated from stereo aerial photographs by Cheryl Hapke, 2003.

Cliff Erosion Rates, Big Sur, CA, Section 6 (PM 21.2-24.2)

by
Cheryl Hapke and Krystal Green

Average erosion rate = 0.17 m/yr (7.0 in/yr)

LEGEND

Coast Highway 1 Postmiles

1994 Cliff Edge

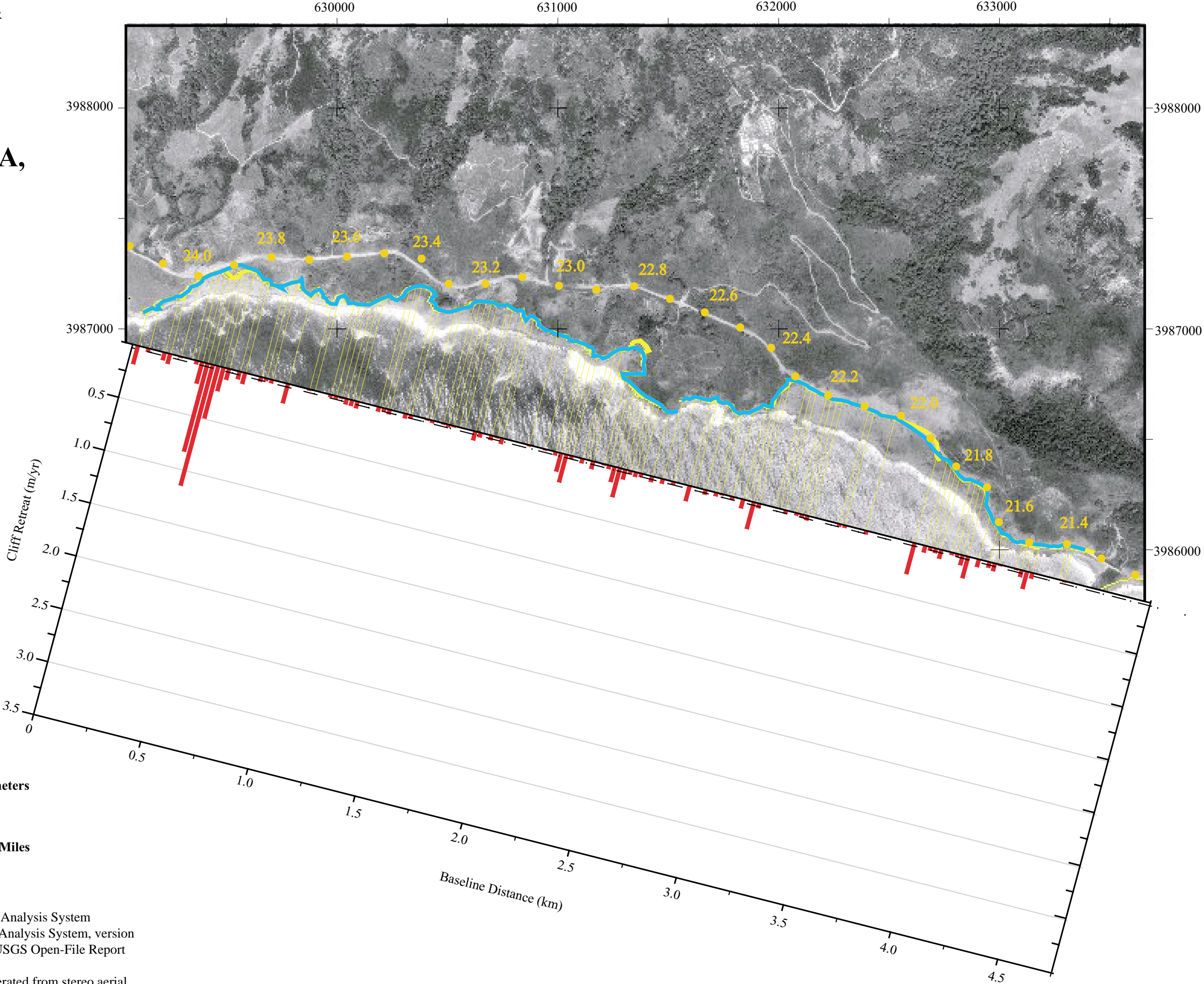
1942 Cliff Edge

Transects

error line




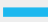
Orthophotograph from USGS DOQ, UTM Zone 10, NAD83.
Transects and erosion rates were generated using the Digital Shoreline Analysis System (Thieler, E. R., Martin, D., and Ergul, A., 2003. The Digital Shoreline Analysis System, version 2.0: Shoreline change measurement software extension for ArcView. USGS Open-File Report 03-076.).
Cliff edges were derived from 1994 and 1942 topographic models generated from stereo aerial photographs by Cheryl Hapke.

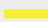



Cliff Erosion Rates
Big Sur, CA
Section 7 (PM 19.2-21.2)
by
Cheryl Hapke and Krystal Green


LEGEND

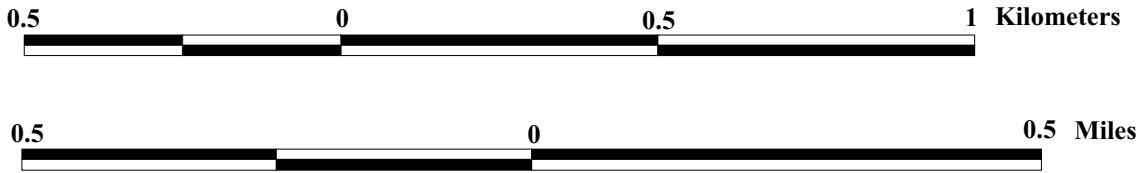

Coast Highway 1
Postmiles


1994 Cliff Edge

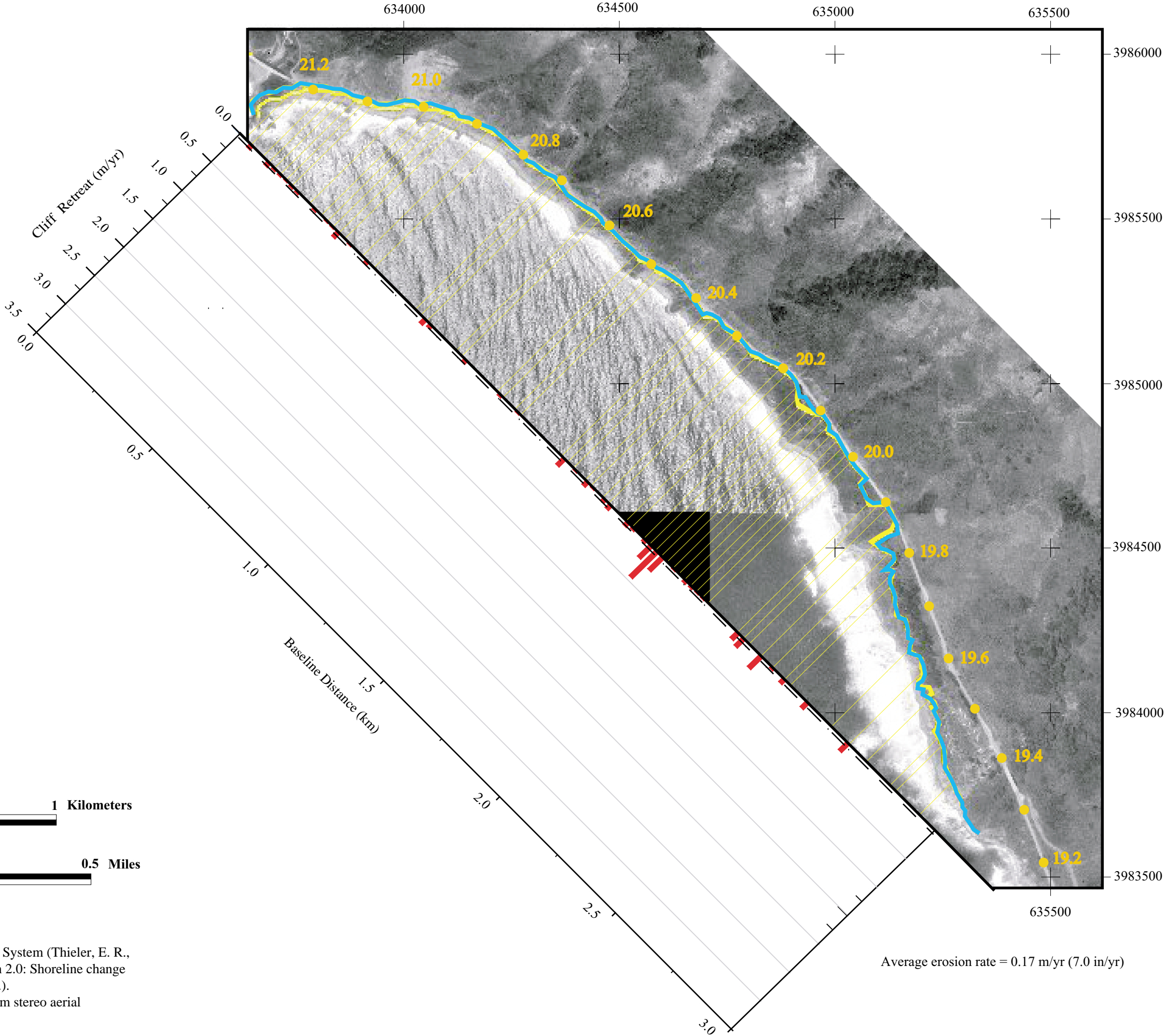

1942 Cliff Edge

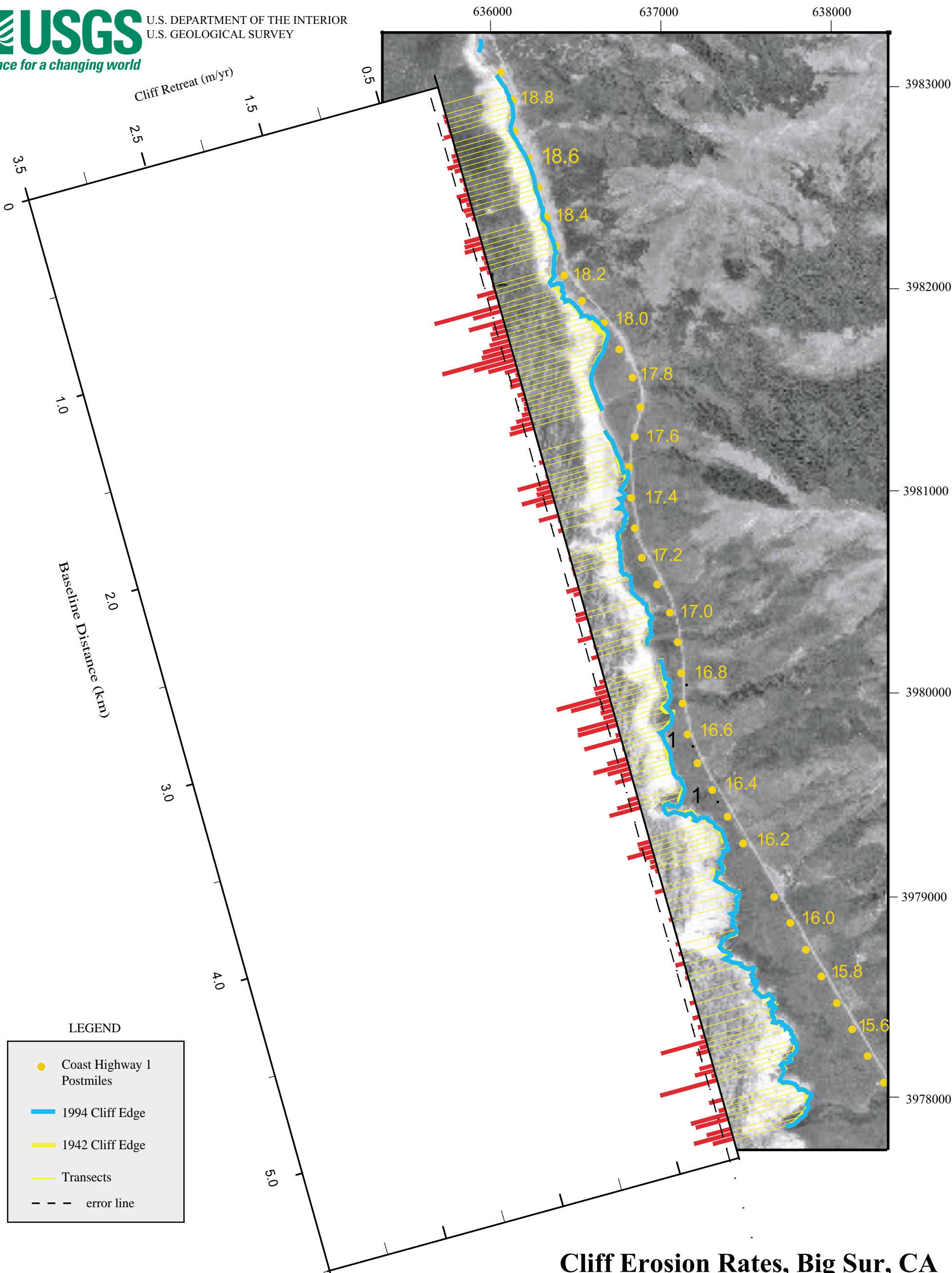

Transects


error line



Orthophotograph from USGS DOQ, UTM Zone 10, NAD83.
 Transects and erosion rates were generated using the Digital Shoreline Analysis System (Thieler, E. R., Martin, D., and Ergul, A., 2003. The Digital Shoreline Analysis System, version 2.0: Shoreline change measurement software extension for ArcView. USGS Open-File Report 03-076.).
 Cliff edges were derived from 1994 and 1942 topographic models generated from stereo aerial photographs by Cheryl Hapke, 2003.

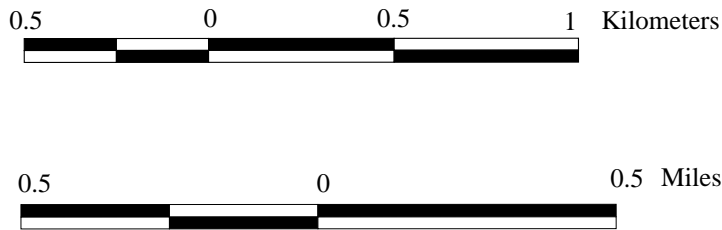




Average erosion rate = 0.2 m/yr (8.0 in/yr)

Cliff Erosion Rates, Big Sur, CA Section 8 (PM 14.0-19.0)

by
Cheryl Hapke, Krystal Green
2003



Orthophotograph from USGS DOQ, UTM Zone 10, NAD83.
Transects and erosion rates were generated using the Digital Shoreline Analysis System (Thieler, E. R., Martin, D., and Ergul, A., 2003. The Digital Shoreline Analysis System, version 2.0: Shoreline change measurement software extension for ArcView. USGS Open-File Report 03-076.).
Cliff edges were derived from 1994 and 1942 topographic models generated from stereo aerial photographs by Cheryl Hapke.

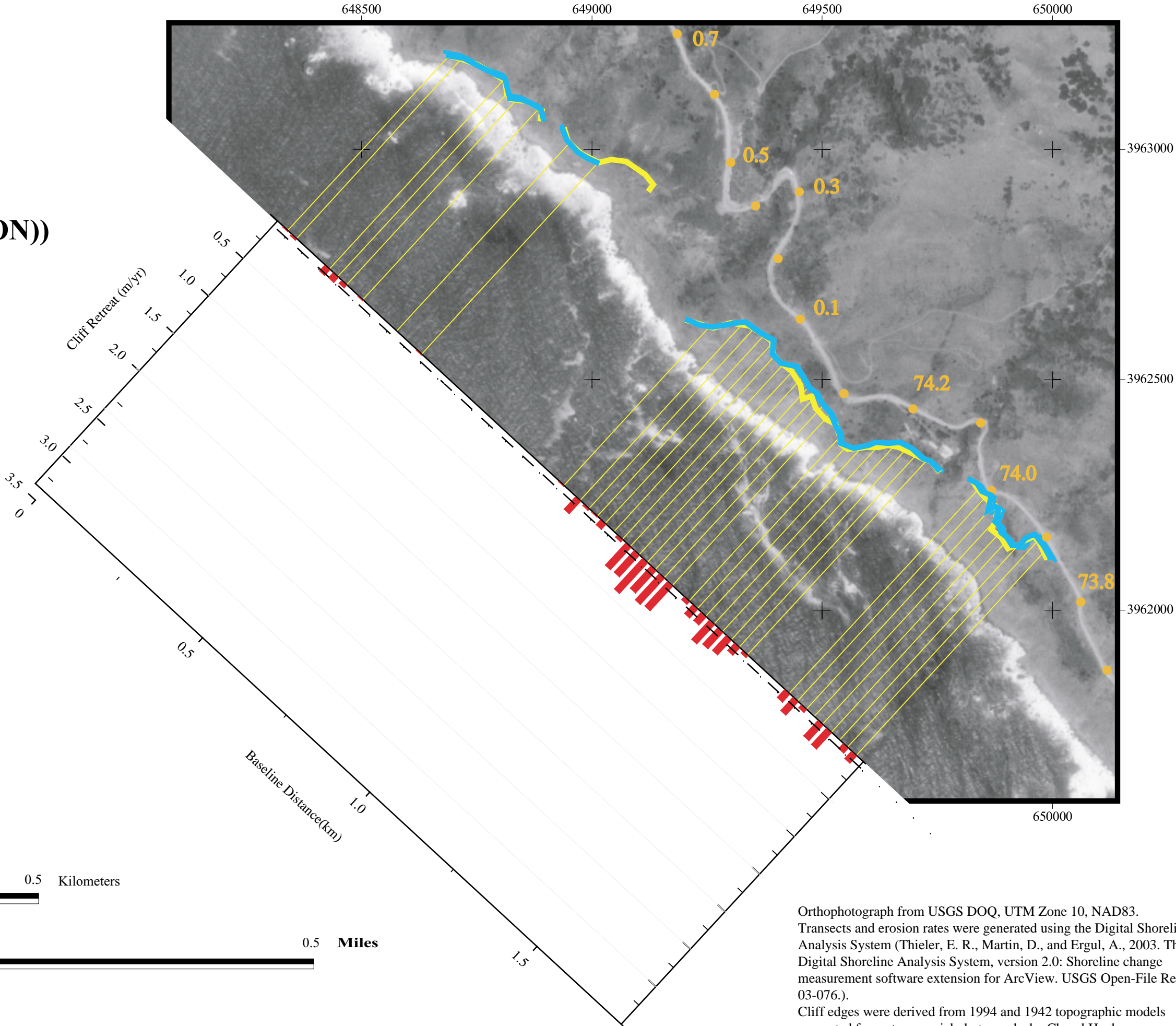
Cliff Erosion Rates
Big Sur, CA
Section 9 (PM 73.0(SLO)-3.5(MON))

by
Cheryl Hapke and Krystal Green

Average erosion rate = 8.2 m/yr (8.0 in/yr)

LEGEND

- Coast Highway 1 Postmiles
- 1994 Cliff Edge
- 1942 Cliff Edge
- Transects
- - - error line



Orthophotograph from USGS DOQ, UTM Zone 10, NAD83.
Transects and erosion rates were generated using the Digital Shoreline Analysis System (Thieler, E. R., Martin, D., and Ergul, A., 2003. The Digital Shoreline Analysis System, version 2.0: Shoreline change measurement software extension for ArcView. USGS Open-File Report 03-076.).
Cliff edges were derived from 1994 and 1942 topographic models generated from stereo aerial photographs by Cheryl Hapke.